

Performance Improvement of Iterative Multiuser Detection for Large Sparsely Spread CDMA Systems by Spatial Coupling

Keigo Takeuchi, *Member, IEEE*, Toshiyuki Tanaka, *Member, IEEE*, and Tsutomu Kawabata, *Member, IEEE*

Abstract—Kudekar *et al.* proved that the belief-propagation (BP) performance for low-density parity check codes can be boosted up to the maximum *a posteriori* (MAP) performance by spatial coupling. In this paper, spatial coupling is applied to sparsely spread code-division multiple-access systems to improve the performance of iterative multiuser detection based on BP. Two iterative receivers based on BP are considered: 1) one receiver is based on exact BP and 2) the other on an approximate BP with Gaussian approximation. The performance of the two BP receivers is evaluated via density evolution (DE) in the dense limit after taking the large-system limit, in which the number of users and the spreading factor tend to infinity while their ratio is kept constant. The two BP receivers are shown to achieve the same performance as each other in these limits. Furthermore, taking a continuum limit for the obtained DE equations implies that the performance of the two BP receivers can be improved up to the performance achieved by the symbol-wise MAP detection, called individually optimal detection, via spatial coupling. Numerical simulations show that spatial coupling can provide a significant improvement in bit-error rate for finite-sized systems especially in the region of high system loads.

Index Terms—Code-division multiple-access (CDMA) systems, sparse spreading, spatial coupling, threshold saturation, iterative multiuser detection, belief propagation, individually-optimal (IO) detection, large-system analysis, density evolution, continuum limit.

I. INTRODUCTION

CODE-DIVISION multiple-access (CDMA) systems have been used in the air interface of third-generation (3G) mobile communication systems [1]–[3]. In CDMA uplink, multiple users simultaneously communicate with one base station in the same frequency band. The base station is required to mitigate multiple-access interference (MAI) to detect the desired signal for each user. Multiuser detection (MUD) is a sophisticated method for mitigating MAI by utilizing the statistical properties of the MAI [4]. Two optimal

receivers were proposed [4]: One optimal receiver, called individually-optimal (IO) receiver, performs the symbol-wise maximum-a-posteriori (MAP) detection. The other optimal receiver, called jointly-optimal (JO) receiver, is based on block-wise MAP detection. Since the two receivers are infeasible in terms of the computational complexity for practical modulation schemes, the main issue in MUD is to construct a suboptimal scheme that can achieve a good tradeoff between performance and complexity.

As suboptimal MUD, linear receivers with low complexity, such as the decorrelator (DEC) [5] and the linear minimum mean-squared error (LMMSE) receiver [6], [7], were proposed. An idealized assumption for analyzing the performance of MUD is random spreading: All spreading sequences have independent and identically-distributed (i.i.d.) elements, whereas pseudo-random sequences are used in practice. The LMMSE receiver for randomly-spread CDMA systems can achieve nearly optimal performance for low system load in the large-system limit [8]–[12], where the number of users K and the spreading factor N tend to infinity while the system load $\beta = K/N$ is kept constant. However, the performance of the LMMSE receiver degrades significantly for moderate-to-high system load, compared to the IO receiver. Thus, it is an important issue to construct a low-complexity scheme that can achieve nearly optimal performance for moderate-to-high system load. The precise meaning of low or high will be noted shortly.

A breakthrough is the use of iterative receivers based on belief propagation (BP) [13], [14]. Iterative receivers are classified into two groups. In one group an iterative receiver performs iterative joint MUD and decoding [15]–[17], in which the detector subtracts the MAI by using decisions fed back from the decoders. In these works, conventional non-iterative detectors were used in iterative MUD and decoding. In the other group an iterative receiver performs MUD with inner iterations [18], in which decisions in the detector are directly utilized to mitigate the MAI. In this paper, we focus on the latter group of iterative receivers, and only consider the uncoded case since coding makes no essential change in analysis of the latter iterative receivers. See [19] for an application of methodology in this paper to the former group of iterative receivers.

Kabashima [18] has proposed a BP-based iterative receiver with Gaussian approximation (GA) for uncoded CDMA systems. It was shown that the proposed receiver achieves nearly optimal performance for moderate system load in

Manuscript received June 26, 2012; revised February 28, 2014; accepted August 21, 2014. Date of publication February 5, 2015; date of current version March 13, 2015. K. Takeuchi was supported in part by the Grant-in-Aid for Young Scientists (B) through the JSPS KAKENHI under Grant 23760329 and in part by the Grant-in-Aid for Young Scientists (A) through the MEXT/JSPS KAKENHI under Grant 26709029. This paper was presented in part at 2011 IEEE International Symposium on Information Theory.

K. Takeuchi and T. Kawabata are with the Department of Communication Engineering and Informatics, University of Electro-Communications, Tokyo 182-8585, Japan (e-mail: ktakeuchi@uec.ac.jp; kawabata@uec.ac.jp).

T. Tanaka is with the Department of Systems Science, Graduate School of Informatics, Kyoto University, Kyoto 606-8501, Japan (e-mail: tt@i.kyotou.ac.jp).

Communicated by A. M. Tulino, Associate Editor for Communications.
Digital Object Identifier 10.1109/TIT.2015.2400445

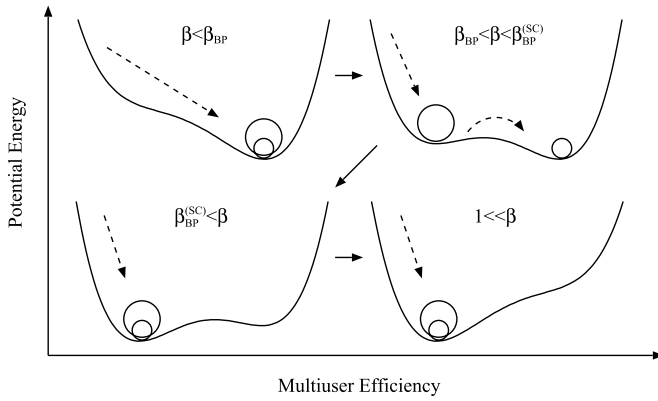


Fig. 1. Landscape of potential energy as a function of multiuser efficiency. The multiuser efficiency for the BP receiver after infinite iterations is represented by the large (respectively resp.) small balls for uncoupled (resp. spatially-coupled) SCDMA systems in the large-sparse-system-limit.

spite of the low complexity. As a method for guaranteeing the convergence of the BP receiver, sparsely-spread CDMA systems, or sparse CDMA (SCDMA) systems, have been considered [20]–[23]. In SCDMA systems the spreading sequence used by each user is sparse: Only c chips out of N chips are non-zero, whereas the conventional CDMA system uses dense spreading sequences whose chips are all non-zero. The main advantage of SCDMA systems is that the convergence of BP-based receivers is guaranteed in the large-system limit with c fixed. Montanari and Tse [20] proved that the performance of an iterative receiver based on exact BP is equal to the performance of the (soft) IO receiver for the conventional (dense) CDMA system below a critical system load β_{BP} , which will be explained shortly, in the large-sparse-system limit, where the dense limit $c \rightarrow \infty$ is taken *after* the large-system limit. Note that the system is sparse even in the dense limit since the large-system limit is taken first. Furthermore, a regular ensemble for sparse spreading sequences has been considered in [22] and [23]. The BP receiver for the regular ensemble can achieve nearly optimal performance for moderate system load.

In order to present the aim of this paper, we shall explain the definition of the critical system load β_{BP} , called the BP threshold in this paper. Let us consider the multiuser efficiency (ME), which is a normalized signal-to-interference ratio (SIR), as a performance measure of MUD. The density-evolution (DE) equations for the BP receiver in the large-sparse-system limit, derived in [20] and [23], characterize the dynamics of the ME. The DE equations can be regarded as a discrete-time gradient system with a potential energy function. Time-evolution of the system represents the dynamics of the ME as the iteration of the BP receiver proceeds. As shown by the potential at the upper left side in Fig. 1, the potential energy as a function of the ME has the unique stable solution for small system load β . As β increases across a critical system load, a metastable solution emerges at an ME value smaller than the original stable solution for high signal-to-noise ratio (SNR), that is, to the left side of the original stable solution, as shown in the potential landscape at the upper right side in Fig. 1. A metastable solution means a stable solution at which the potential energy is minimized locally, whereas a global stable

solution means a global minimizer of the potential energy. The BP threshold β_{BP} is defined as the supremum of β_{th} such that the BP receiver can achieve the ME corresponding to the rightmost¹ stable solution after infinite iterations for all $\beta \in (0, \beta_{th})$. Note that the infinite-iteration limit is considered *after* the large-sparse-system limit. The BP threshold β_{BP} is characterized as the bifurcation point at which the stability of the potential energy changes: The potential energy has one stable solution for $\beta < \beta_{BP}$, whereas it has two stable solutions and one unstable solution for $\beta > \beta_{BP}$. In fact, the ME for the BP receiver converges to the unique stable solution after infinite iterations for $\beta < \beta_{BP}$. For $\beta > \beta_{BP}$, on the other hand, the ME converges to the left stable solution after infinite iterations, since the initial ME is commonly a smaller value than the unstable solution (See the large balls in Fig. 1). Thus, the BP threshold β_{BP} is equal to the bifurcation point between the monostability and the bistability.

The aim of this paper is to construct a novel SCDMA system that improves the BP threshold β_{BP} . For that purpose, we utilize a recent excellent achievement on coding theory: Kudekar et al. [24] have proved that the BP threshold of a low-density parity-check (LDPC) convolutional code [25] over the binary erasure channel (BEC) is equal to the MAP threshold of the corresponding LDPC block code (See also [26]). Since an LDPC convolutional code can be regarded as a spatially-coupled (SC) chain of LDPC block codes, this result was referred to as “threshold saturation via spatial coupling” [24]. An improvement of the BP threshold via spatial coupling is believed to be a universal phenomenon [27]–[32]. The same phenomenon has been observed in many other problems [33]–[47]. In this paper, we propose spatially-coupled SCDMA (SC-SCDMA) systems to improve the BP threshold.

We shall develop a simple and generic method for characterizing the position of the BP threshold for SC-SCDMA systems by using a potential for the corresponding *uncoupled* system. In this paper, potential for the uncoupled system is simply referred to as potential, since potential for the coupled system is not considered. Recently, we have presented a phenomenological study on threshold improvement via spatial coupling [29]. The study allows us to specify a (probably tight) lower bound on the BP threshold $\beta_{BP}^{(SC)}$ for SC-SCDMA systems via the shape of a potential energy function: The BP threshold is larger than or equal to a system load $\tilde{\beta}_{BP}^{(SC)} (> \beta_{BP})$, called potential threshold, at which the heights of the potential energy at the two stable solutions coincide with each other. The ME for $\beta < \tilde{\beta}_{BP}^{(SC)}$ converges to the right stable solution after infinite iterations, whereas the ME for $\beta > \tilde{\beta}_{BP}^{(SC)}$ may be trapped in the other stable solution (See the small balls in Fig. 1). Thus, the BP receiver for SC-SCDMA systems can achieve better performance than that for the corresponding uncoupled SCDMA system in the large-sparse-system limit, when the system load is between β_{BP} and $\tilde{\beta}_{BP}^{(SC)}$. The main contribution of this paper is to prove that the lower bound $\tilde{\beta}_{BP}^{(SC)}$ is equal to

¹If the potential energy is monostable, the rightmost stable solution corresponds to the unique stable solution.

a critical threshold β_{IO} for the uncoupled CDMA system, called the IO threshold in this paper.

The IO threshold $\beta_{\text{IO}} (> \beta_{\text{BP}})$ has been specified via the large-system analysis of the IO receiver based on the non-rigorous replica method [10]. The ME of the IO receiver for the uncoupled CDMA system is characterized via essentially the same potential energy as that for determining the conventional BP threshold β_{BP} . The IO threshold β_{IO} is defined as the system load at which the heights of the potential energy at the two stable solutions coincide with each other. The ME achieved by the IO receiver corresponds to the rightmost stable solution of the potential energy for $\beta < \beta_{\text{IO}}$, whereas it corresponds to the left stable solution for $\beta > \beta_{\text{IO}}$.

In summary, the BP receiver for the uncoupled SCDMA system is inferior to the IO receiver for system loads between β_{BP} and β_{IO} , since the definition of the BP threshold β_{BP} implies that the ME achieved by the BP receiver corresponds to the left stable solution of the potential energy for $\beta > \beta_{\text{BP}}$. On the other hand, we will show that the potential threshold $\tilde{\beta}_{\text{BP}}^{(\text{SC})}$ is equal to the IO threshold β_{IO} , by proving that the potential for characterizing $\tilde{\beta}_{\text{BP}}^{(\text{SC})}$ is essentially the same as for determining β_{IO} . Thus, the BP receiver for SC-SCDMA systems can achieve the same performance as the IO receiver for the uncoupled CDMA system when β is smaller than β_{IO} . In this paper, small system load means that β is smaller than one. We refer to SCDMA systems as moderately loaded systems if β is between one and the conventional BP threshold β_{BP} . High system load means that β is between the conventional BP threshold β_{BP} and the IO threshold β_{IO} .

We have so far focused on the thresholds in the large-sparse-system limit. It is worth investigating what they indicate for the performance of finite-sized systems. The definition of the BP threshold β_{BP} implies that the asymptotic ME changes discontinuously at $\beta = \beta_{\text{BP}}$ as β grows. What does this phenomenological picture indicate for finite-sized systems? The ME for the BP receiver never changes discontinuously for finite-sized systems. Rather, numerical simulations in [18] and [20] implied that the ME decreases rapidly like a waterfall when the system load moves from below to above the BP threshold β_{BP} . The slope of the ME as a function of β becomes steep around the critical point $\beta = \beta_{\text{BP}}$ as the system size grows. Thus, the system size required for achieving an ME close to the asymptotic one increases as the system load gets closer to the BP threshold β_{BP} from below. In other words, the performance for a fixed finite-sized system gets away from the asymptotic one as the system load gets closer to the BP threshold. These arguments may indicate that increasing the BP threshold results in improving the performance for a fixed finite-sized system. Numerical simulations will show that spatial coupling can improve the performance of the BP receiver for a finite-sized system especially in the region of high system loads.

We would like to refer to an independent work [41], [42]: Schlegel and Truhachev proposed another SC-SCDMA system based on graph lifting, while we consider sparse spreading [43]. Interestingly, the obtained DE equations are

the same as those derived in this paper. They analyzed the BP threshold for the coupled case in the high SNR limit, whereas we investigate its position for *any* SNR.

The rest of this paper is organized as follows: After summarizing the notation used in this paper, we first consider the conventional SCDMA system in Section II. After introducing its factor-graph representation, SC-SCDMA systems are defined on the basis of two operations with respect to the factor graph. In Section III two BP-based iterative receivers are derived. One receiver is based on exact BP [20], [23], and the other receiver is a BP receiver with GA [18]. Section IV presents the main results of this paper. The main theorem on spatial coupling is proved as a general framework in Section V. The section is organized as an independent section, so that it should be possible to skip Sections II–IV and to read Section V. In Section VI the performance of the SC-SCDMA systems is investigated numerically. Section VII concludes this paper.

A. Notation

For a matrix \mathbf{A} , \mathbf{A}^T denotes the transpose of \mathbf{A} . \mathbf{I}_N stands for the $N \times N$ identity matrix. The Kronecker delta is denoted by $\delta_{i,j}$. For a natural number L and an integer l , the remainder $(l)_L = l \bmod L$ for the division of l by L is equal to $l + kL$ for an integer k such that $0 \leq l + kL \leq L - 1$.

For a random variable x , $\mathbb{E}[x]$ and $\mathbb{V}[x]$ denote the mean and variance of x , respectively. The notation $p(x)$ stands for the probability density function (pdf) of a continuous random variable x . We use the same notation $p(x)$ for the probability mass function (pmf) of a discrete random variable x . The notation $x \sim p(x)$ indicates that the pdf or pmf of a random variable x is equal to $p(x)$. The real Gaussian pdf with a mean vector \mathbf{m} and a covariance matrix $\mathbf{\Sigma}$ is denoted by $\mathcal{N}(\mathbf{m}, \mathbf{\Sigma})$. In particular, the pdf for a zero-mean Gaussian random variable x with variance σ^2 is written as

$$g(x; \sigma^2) = \frac{1}{\sqrt{2\pi\sigma^2}} \exp\left(-\frac{x^2}{2\sigma^2}\right). \quad (1)$$

For variables $\{a_k \in \mathcal{M}\}$ on a finite alphabet \mathcal{M} , the sum $\sum_{\{a_k\}} f(\{a_k\})$ denotes the marginalization with respect to $\{a_k\}$ —the summation of a function $f(\{a_k\})$ over all possible configurations of $\{a_k\}$. Furthermore, the sum $\sum_{\setminus a_k}$ stands for the summation over all possible configurations of $\{a_{k'}\}$ except for a_k . For a conditional pdf or pmf $p(x|y)$, $p(x|y) \propto f(x)$ means that $p(x|y)$ is proportional to $f(x)$, i.e. there is an x -independent constant $C(y)$ such that $p(x|y) = C(y)f(x)$.

Graphs with nodes specified by two indices i and j are considered for SC systems. Thus, the pair (i, j) represents not an edge but a node for the SC systems. Furthermore, $\partial(i, j)$ stands for the neighborhood of the node (i, j) , i.e. the set of nodes that are directly connected to the node (i, j) .

II. SYSTEM MODEL

A. Sparsely-Spread CDMA Systems

We introduce conventional synchronous SCDMA systems before presenting SC-SCDMA systems. In this paper, the receive power is assumed to be identical for all users.

Let K and N denote the number of users and the spreading factor, respectively. Without loss of generality, we focus on one symbol period. User k sends the product of the unbiased binary phase shift keying (BPSK) data symbol $b_k \in \{-1, 1\}$ and a sparse spreading sequence $\mathbf{s}_k = (s_{1,k}, \dots, s_{N,k})^T$ with $\bar{c}_k = \mathbb{E}[\|\mathbf{s}_k\|^2]$, in which the statistics of $\{\mathbf{s}_k\}$ will be defined shortly. Under the assumption of unfaded channels, the received vector $\mathbf{y} = (y_1, \dots, y_N)^T \in \mathbb{R}^N$ is given by

$$\mathbf{y} = \sum_{k \in \mathcal{K}} \frac{1}{\sqrt{\bar{c}_k}} \mathbf{s}_k b_k + \mathbf{w}, \quad (2)$$

with $\mathcal{K} = \{1, \dots, K\}$. In (2), the N -dimensional vector $\mathbf{w} \sim \mathcal{N}(0, \sigma_n^2 \mathbf{I}_N)$ denotes additive white Gaussian noise (AWGN) with variance σ_n^2 . The expression (2) can be re-written as

$$\mathbf{y} = \mathbf{S}\mathbf{b} + \mathbf{w}, \quad (3)$$

with $\mathbf{S} = (\bar{c}_1^{-1/2} \mathbf{s}_1, \dots, \bar{c}_K^{-1/2} \mathbf{s}_K)$ and $\mathbf{b} = (b_1, \dots, b_K)^T$.

The conventional CDMA systems use dense spreading sequences whose elements are all non-zero. In the SCDMA system (2), on the other hand, user k utilizes the sparse spreading sequence \mathbf{s}_k with c_k ($\ll N$) non-zero elements. The number c_k is equal to the weight (number of non-zero elements) of the k th column of the spreading matrix \mathbf{S} . For simplicity, we assume sparse spreading with binary antipodal chips as non-zero chips: Non-zero elements of \mathbf{s}_k take ± 1 with equal probability. Then, the normalization constant $\bar{c}_k = \mathbb{E}[\|\mathbf{s}_k\|^2]$ is equal to the average of the k th column weight of \mathbf{S} . Let r_n denote the n th row weight for the spreading matrix \mathbf{S} . A constraint with respect to the number of non-zero elements imposes $\sum_{k=1}^K c_k = \sum_{n=1}^N r_n$. In this paper, we only consider regular and quasi-regular ensembles of spreading matrices.

Example 1 (Regular Ensemble): In the (c, r) -regular ensemble of \mathbf{S} , all column weights $\{c_k\}$ and all row weights $\{r_n\}$ are equal to c and r , respectively. The constraint $\sum_{k=1}^K c_k = \sum_{n=1}^N r_n$ implies that K and N must satisfy the constraint on the system load $\beta = K/N = r/c$. One regular spreading matrix is obtained as follows:

- 1) Pick up a matrix from all possible binary (0 or 1) matrices with row weight r and column weight c uniformly and randomly.
- 2) Replace each non-zero element of the obtained binary matrix by $\pm c^{-1/2}$ independently and with equal probability.

The (c, r) -regular ensemble of spreading matrices is composed of all possible spreading matrices obtained in the above-mentioned manner.

The (c, r) -regular ensemble is well-defined when K and N satisfy the constraint on the system load $\beta = r/c$. The following r -quasi-regular ensemble is well-defined for any K and N .

Example 2 (Quasi-Regular Ensemble): In the r -quasi-regular ensemble, all row weights $\{r_k\}$ are fixed to r . Let $N_w = rN$ denote the number of non-zero elements in \mathbf{S} . The column vectors of \mathbf{S} are classified into two groups with column weights $c = \lfloor N_w/K \rfloor$ and $c + 1$: One group

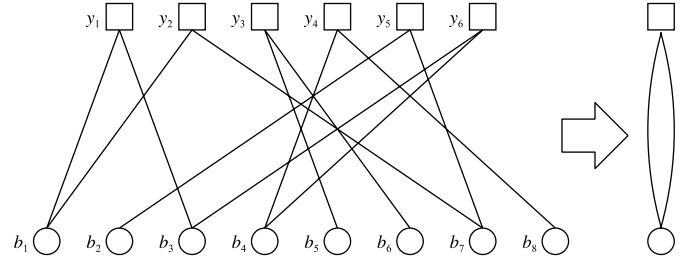


Fig. 2. An example of the factor graph picked up from the 2-quasi-regular ensemble for $K = 8$ and $N = 6$ (left). The graph on the right represents a simplified graph representation for the same ensemble.

consists of $(N_w - cK)$ column vectors with weight $c + 1$. The other group is composed of the remaining column vectors with weight c . The average column weight \bar{c} is given by $\bar{c} = r/\beta$. It is straightforward to confirm that the constraint $N_w = \sum_{k=1}^K c_k$ is satisfied. One spreading matrix is obtained as follows: A binary matrix is uniformly and randomly picked up from all possible binary matrices satisfying the conditions above. Subsequently, the gain $\pm \bar{c}^{-1/2}$ is associated with each non-zero element of the obtained binary matrix independently and with equal probability. The r -quasi-regular ensemble of spreading matrices consists of all possible spreading matrices obtained in this manner.

Obviously, the r -quasi-regular ensemble reduces to the $(rN/K, r)$ -regular ensemble when $N_w = rN$ is a multiple of K . Thus, we only consider the quasi-regular ensemble in this paper.

B. Factor Graph Representation

We next introduce the factor-graph representation [14] for the SCDMA system (2), shown in Fig. 2. Each data symbol b_k corresponds to a variable node represented by a circle, whereas each received signal y_n is associated with a function node shown by a square. If the n th chip $s_{n,k}$ for user k is non-zero, there exists an edge connecting function node n and variable node k in the factor graph. Furthermore, the edge is associated with the corresponding gain $\bar{c}_k^{-1/2} s_{n,k}$. Let $\partial k \subset \mathcal{N} = \{1, \dots, N\}$ denote the neighborhood of variable node k , i.e. the set of function nodes that are directly connected to variable node k . The degree $|\partial k|$ of variable node k corresponds to the k th column weight c_k of the spreading matrix \mathbf{S} . Similarly, let $\partial n \subset \mathcal{K}$ denote the neighborhood of function node n . The degree $|\partial n|$ of function node n is equal to the n th row weight r_n of the spreading matrix.

There is a one-to-one correspondence between a spreading matrix and a factor graph. Thus, we can consider an ensemble of factor graphs corresponding to the r -quasi-regular ensemble of spreading matrices. This ensemble is referred to as the r -quasi-regular ensemble of factor graphs in this paper, or simply as the r -quasi-regular ensemble if it is obvious that the ensemble is an ensemble of factor graphs.

The crucial property of factor graphs picked up from the r -quasi-regular ensemble is the asymptotic cycle-free (ACF) property in the large-system limit, where K and N tend to infinity while the system load $\beta = K/N$ is kept constant. The length of a cycle is defined as the number of edges

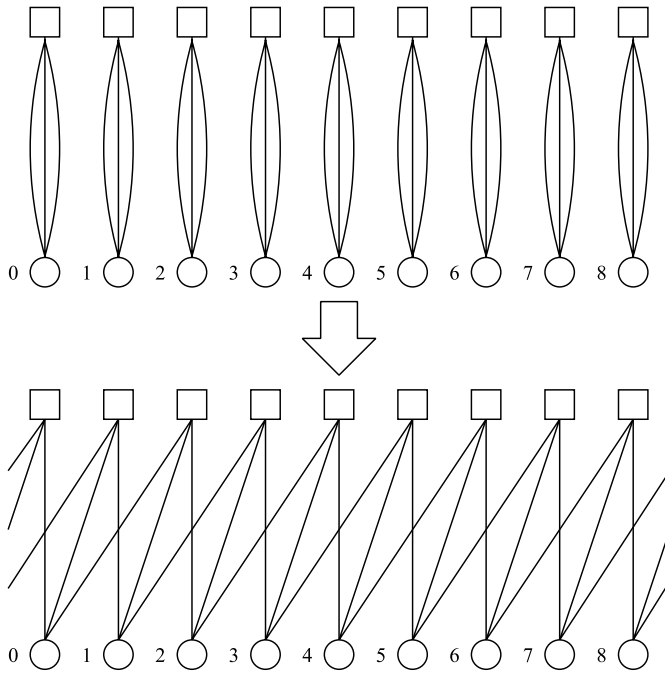


Fig. 3. Spatial coupling for $r = 3$, $L = 9$, and $W = 2$.

included in the cycle. A factor graph picked up from the r -quasi-regular ensemble has no cycles with *finite* length with probability one in the large-system limit [14], [20], [23]. This ACF property guarantees the convergence of iterative detection based on BP in the large-system limit.

C. Spatial Coupling

In this section, we present an intuitive explanation for spatial coupling as a brief introduction, instead of presenting a precise definition of SC-SCDMA systems. The precise definition will be presented in the next section. We use a simplified graph representation for the r -quasi-regular ensemble (See the graph on the right in Fig. 2). The graph consists of one function node represented by a square and of one variable node shown by a circle. The number of edges is equal to the degree r of the function nodes in the original factor graph. In other words, the simplified graph only represents the fact that the degree of the function nodes is equal to r . In introducing SC-SCDMA systems, multiple simplified graphs are used. Thus, we refer to each simplified graph as a subgraph. An SC-SCDMA system with coupling width W and the number of subgraphs L is constructed from two operations with respect to the simplified graph representation.

- 1) Generate L uncoupled subgraphs. Different subgraphs may have different spreading factors.
- 2) Disconnect $Wr/(W+1)$ edges out of r edges from the variable node at position l for $l = 0, \dots, L-1$. Subsequently, reconnect $r/(W+1)$ edges out of the disconnected edges to the variable nodes at position $(\tilde{l}')_L$ for $\tilde{l}' = l - W, \dots, l - 1$ (See Fig. 3). The subgraphs are connected circularly.

The degree of the function nodes r is restricted to a multiple of $W+1$. In Step 2, L subgraphs have been coupled circularly, whereas Kudekar et al. [24] considered termination at both ends. The point of spatial coupling is that the data symbols at

both ends are known to the receiver or can be detected well. Reliable information about the data symbols at both ends is expected to spread over the whole system by spatial coupling.

In order to allow the receiver to detect the data symbols at both ends, we reduce the system loads for positions $l = 0, \dots, W-1$. It would be possible to send known symbols in these positions instead. This scheme is equivalent to assuming noiseless channels with zero system load for the positions. We use small system load to reduce the influence of rate loss in the case of finite L . In the next section, we present the detailed definition of SC-SCDMA systems.

D. Spatially-Coupled SCDMA Systems

MUD for SC-SCDMA systems is performed for every L symbol periods,² whereas it is done for every symbol period in the conventional SCDMA system (2). This implies that the detection delay increases linearly in L for SC-SCDMA systems. In practice, the detection delay does not necessarily result in the overall delay for coded systems: If L is smaller than the code length, the overall delay is dominated by the delay due to decoding.

Let N_l denote the spreading factor in symbol period l . The received vector $\mathbf{y}_l = (y_{1,l}, \dots, y_{N_l,l})^T \in \mathbb{R}^{N_l}$ in symbol period l is given by

$$\mathbf{y}_l = \sum_{k \in \mathcal{K}} \sum_{l' \in \mathcal{L}} \frac{1}{\sqrt{\tilde{c}_{l,k,l'}}} h_{(l-l')_L} s_{l,k,l'} b_{k,l'} + \mathbf{w}_l, \quad (4)$$

for $l \in \mathcal{L} = \{0, \dots, L-1\}$, with

$$h_l = \begin{cases} 1/\sqrt{W+1} & \text{for } l = 0, \dots, W \\ 0 & \text{for } l = W+1, \dots, L-1. \end{cases} \quad (5)$$

In (4), the vector $\mathbf{w}_l \sim \mathcal{N}(\mathbf{0}, \sigma_n^2 \mathbf{I}_{N_l})$ denotes the AWGN vector with variance σ_n^2 . The N_l -dimensional vector $\mathbf{s}_{l,k,l'} = (s_{1,l,k,l'}, \dots, s_{N_l,l,k,l'})^T$ represents the l' th sparse spreading sequence of user k for symbol period l , which will be defined shortly. The normalization constant $\tilde{c}_{l,k,l'}$ is given by $\tilde{c}_{l,k,l'} = \mathbb{E}[\|\mathbf{s}_{l,k,l'}\|^2]$. Finally, $b_{k,l} \in \{-1, 1\}$ denotes the l th BPSK data symbol for user k . Let $\mathbf{b}_l = (b_{1,l}, \dots, b_{K,l})^T$ and $\mathbf{S}_{l,l'} = (\tilde{c}_{l,1,l'}^{-1/2} s_{l,1,l'}, \dots, \tilde{c}_{l,K,l'}^{-1/2} s_{l,K,l'})$. The system (4) can be represented as

$$\begin{bmatrix} \mathbf{y}_0 \\ \vdots \\ \mathbf{y}_{L-1} \end{bmatrix} = \frac{1}{\sqrt{W+1}} \mathbf{G} \begin{bmatrix} \mathbf{b}_0 \\ \vdots \\ \mathbf{b}_{L-1} \end{bmatrix} + \begin{bmatrix} \mathbf{w}_0 \\ \vdots \\ \mathbf{w}_{L-1} \end{bmatrix}, \quad (6)$$

with

$$\mathbf{G} = \begin{bmatrix} \mathbf{S}_{0,0} & & \mathbf{S}_{0,L-W} & \cdots & \mathbf{S}_{0,L-1} \\ \vdots & \ddots & & \ddots & \vdots \\ \vdots & & \ddots & & \mathbf{S}_{W-1,L-1} \\ \mathbf{S}_{W,0} & & & \ddots & \\ \vdots & \ddots & & & \\ \mathbf{S}_{L-1,L-W-1} & \cdots & \cdots & \mathbf{S}_{L-1,L-1} \end{bmatrix}. \quad (7)$$

²Temporal coupling may be an appropriate naming, rather than spatial coupling. Nonetheless, we follow [24] to use the term “spatial coupling” in this paper.

It is straightforward to confirm that the simplified graph representation in Fig. 3 corresponds to the one for the SC-SCDMA system with $r = 3$, $L = 9$, and $W = 2$.

We reduce the system loads for positions $l = 0, \dots, W - 1$. This corresponds to the situation under which the SC-SCDMA system (4) has two phases: initialization and communication phases. The spreading factors N_l for the initialization phase $l = 0, \dots, W - 1$ are fixed to a large value N_{init} to allow the receiver to detect the data symbols transmitted in the phase. On the other hand, the spreading factors N_l for the communication phase $l = W, \dots, L - 1$ are set to a small value N to increase the sum rate.

The average system load $\bar{\beta}$ of the SC-SCDMA system is given by

$$\begin{aligned}\bar{\beta} &= \frac{KL}{N_{\text{init}}W + N(L - W)} \\ &= \frac{1}{\beta_{\text{init}}^{-1}(W/L) + \beta^{-1}\{1 - (W/L)\}},\end{aligned}\quad (8)$$

where $\beta_{\text{init}} = K/N_{\text{init}}$ and $\beta = K/N$ denote the system loads for the initialization and communication phases, respectively. The average system load (8) converges to the system load β for the conventional SCDMA system (2) when $\gamma = W/L$ tends to zero.

We only consider the quasi-regular ensemble with spatial coupling. Throughout this paper, the matrix (7) is assumed to be drawn from the (r, L, W) -quasi-regular ensemble below.

Example 3 (Quasi-Regular Ensemble With Spatial Coupling): In the (r, L, W) -quasi-regular ensemble with spatial coupling, all row weights of the matrix (7) are fixed to r . Each non-zero submatrix $\mathbf{S}_{l,l'}$ has the row weight $r/(W + 1)$ for all rows. Thus, the row weight r of (7) must be a multiple of $W + 1$. Each submatrix $\mathbf{S}_{l,l'}$ is a member of the $r/(W + 1)$ -quasi-regular ensemble with the number of users K and the spreading factor N_l , presented in Example 2. The average column weights $\{\bar{c}_{l,k,l'}\}$ are equal to $\bar{c}_{l,k,l'} = r/\{(W + 1)\beta_{\text{init}}\}$ for the initialization phase $l = 0, \dots, W - 1$ and $\bar{c}_{l,k,l'} = r/\{(W + 1)\beta\}$ for the communication phase $l = W, \dots, L - 1$. The (r, L, W) -ensemble consists of all possible matrices (7) that satisfy the conditions above. It is guaranteed that the (r, L, W) -ensemble of factor graphs corresponding to the (r, L, W) -ensemble of (7) has the ACF property in the large-system limit, although its proof is omitted.

III. ITERATIVE RECEIVERS

A. Belief Propagation

The goal of the receiver is to compute the marginal posterior probability for each data symbol $b_{k,l'}$, given by

$$p(b_{k,l'}|\mathcal{Y}, \mathbf{G}) = \sum_{\mathcal{B}} p(\mathcal{B}|\mathcal{Y}, \mathbf{G}), \quad (9)$$

where the joint posterior probability $p(\mathcal{B}|\mathcal{Y}, \mathbf{G})$ of $\mathcal{B} = \{b_{l'} : l' \in \mathcal{L}\}$ given $\mathcal{Y} = \{y_l : l \in \mathcal{L}\}$ and \mathbf{G} is defined as

$$p(\mathcal{B}|\mathcal{Y}, \mathbf{G}) = \frac{p(\mathcal{Y}|\mathbf{G}, \mathcal{B})p(\mathcal{B})}{p(\mathcal{Y}|\mathbf{G})}, \quad (10)$$

with

$$p(\mathcal{Y}|\mathbf{G}) = \sum_{\mathcal{B}} p(\mathcal{Y}|\mathbf{G}, \mathcal{B})p(\mathcal{B}). \quad (11)$$

In (10), the conditional pdf $p(\mathcal{Y}|\mathbf{G}, \mathcal{B})$ represents the SC-SCDMA system (6). It is well-known that the IO decision $\hat{b}_{k,l'}^{(\text{IO})} = \arg\max_{b_{k,l'} \in \{-1, 1\}} p(b_{k,l'}|\mathcal{Y}, \mathbf{G})$ and the soft IO decision $\hat{b}_{k,l'}^{(\text{SIO})} = \sum_{b_{k,l'} \in \{-1, 1\}} b_{k,l'} p(b_{k,l'}|\mathcal{Y}, \mathbf{G})$ minimize the bit error rate (BER) and the mean-squared error (MSE), respectively [4].

BP is an iterative algorithm for computing the marginal posterior probability (9) efficiently. Messages are exchanged between the variable and function nodes on the factor graph for the SC-SCDMA system (4). Let $q_{n,l}^{(i)}(b_{k,l'})$ (resp. $m_{n,l}^{(i)}(b_{k,l'})$) denote the message passed from the function node $y_{n,l}$ (resp. variable node $b_{k,l'}$) to the variable node $b_{k,l'}$ (resp. function node $y_{n,l}$) in iteration i . A tentative marginal posterior probability of $b_{k,l'}$ in iteration i is given by the product of all incoming messages to the variable node $b_{k,l'}$,

$$p^{(i)}(b_{k,l'}|\mathcal{Y}, \mathbf{G}) \propto \prod_{(\tilde{n}, \tilde{l}) \in \partial(k, l')} q_{\tilde{n}, \tilde{l}}^{(i)}(b_{k,l'}), \quad (12)$$

where the set of index pairs $\partial(k, l') \subset \mathcal{N}_{\text{max}} \times \mathcal{L}$, with $\mathcal{N}_{\text{max}} = \{1, \dots, \max_l N_l\}$, denotes the neighborhood of the variable node $b_{k,l'}$. The BP decision is defined as the hard (or soft) decision based on the marginal posterior probability (12) in each iteration.

The messages $q_{n,l}^{(i)}(b_{k,l'})$ and $m_{n,l}^{(i)}(b_{k,l'})$ are updated as follows:

$$\begin{aligned}q_{n,l}^{(i)}(b_{k,l'}) &= \sum_{\mathcal{B}} p\left(y_{n,l} \left| \sum_{(\tilde{k}, \tilde{l}) \in \partial(n, l)} \frac{s_{n,l,\tilde{k},\tilde{l}} b_{\tilde{k},\tilde{l}}}{\sqrt{(W + 1)\bar{c}_{l,\tilde{k},\tilde{l}}}} \right. \right) \\ &\quad \cdot \prod_{(\tilde{k}, \tilde{l}) \in \partial(n, l) \setminus (k, l')} m_{n,l}^{(i-1)}(b_{\tilde{k},\tilde{l}}),\end{aligned}\quad (13)$$

$$m_{n,l}^{(i)}(b_{k,l'}) = \alpha_{n,l,k,l'}^{(i)} \prod_{(\tilde{n}, \tilde{l}) \in \partial(k, l') \setminus (n, l)} q_{\tilde{n}, \tilde{l}}^{(i)}(b_{k,l'}), \quad (14)$$

with the initial values $m_{n,l}^{(0)}(b_{k,l'}) = 1/2$. In (13), the set of index pairs $\partial(n, l) \subset \mathcal{K} \times \mathcal{L}$ denotes the neighborhood of the function node $y_{n,l}$. Furthermore, the conditional pdf in (13) represents the SC-SCDMA system (4) for the n th received signal in symbol period l . In (14), $\alpha_{n,l,k,l'}^{(i)}$ denotes the normalization constant. We hereafter refer to the update rules (13) and (14) as the sum and product steps, respectively.

It is known that BP computes the exact marginal posterior probabilities if there are no cycles in the factor graph [13]. When the factor graphs have cycles, the convergence of BP is not guaranteed in general. Even if BP has converged, the computed marginal posterior probabilities (12) are approximate. Fortunately, the (r, L, W) -ensemble of factor graphs has the ACF property in the large-system limit: There are no cycles with finite length in the large-system limit. Thus, the BP receiver (12) is guaranteed to converge in the infinite-iteration limit $i \rightarrow \infty$ after taking the large-system limit. Note that the two limits do not commute with each other.

B. Gaussian Approximation

The computational complexity of the BP receiver is exponential in the row weight r , whereas the complexity is linear in K and L . Consequently, a large row weight r cannot be used in terms of the complexity. We derive an approximate BP-based iterative receiver that works efficiently for large r , following [18]. The update rule (13) can be regarded as a marginalization with respect to the independent variables $b_{\tilde{k},\tilde{l}'} \sim m_{n,l}^{(i)}(b_{\tilde{k},\tilde{l}'})$ for all $(\tilde{k},\tilde{l}') \in \partial(n,l) \setminus (k,l')$. Let us define the postulated interference to the data symbol $b_{k,l'}$ in the function node $y_{n,l}$ as

$$\tilde{l}_{n,l,k,l'}^{(i)} = \sum_{(\tilde{k},\tilde{l}') \in \partial(n,l) \setminus (k,l')} \frac{s_{n,l,\tilde{k},\tilde{l}'} \tilde{b}_{\tilde{k},\tilde{l}'}^{(i)}}{\sqrt{(W+1)\tilde{c}_{l,\tilde{k},\tilde{l}'}}}, \quad (15)$$

where $\tilde{b}_{\tilde{k},\tilde{l}'}^{(i)} \sim m_{n,l}^{(i)}(b_{\tilde{k},\tilde{l}'})$. The central limit theorem implies that the interference (15) converges in law to a Gaussian random variable in the limit $|\partial(n,l)| = r \rightarrow \infty$. The mean $\tilde{\mu}_{n,l,k,l'}^{(i)}$ and variance $\tilde{v}_{n,l,k,l'}^{(i)}$ of (15) are given by

$$\begin{aligned} \tilde{\mu}_{n,l,k,l'}^{(i)} &= \sum_{(\tilde{k},\tilde{l}') \in \partial(n,l) \setminus (k,l')} \frac{s_{n,l,\tilde{k},\tilde{l}'} \mathbb{E}[\tilde{b}_{\tilde{k},\tilde{l}'}^{(i)}]}{\sqrt{(W+1)\tilde{c}_{l,\tilde{k},\tilde{l}'}}}, \\ \tilde{v}_{n,l,k,l'}^{(i)} &= \sum_{(\tilde{k},\tilde{l}') \in \partial(n,l) \setminus (k,l')} \frac{s_{n,l,\tilde{k},\tilde{l}'}^2 \mathbb{E}[(\tilde{b}_{\tilde{k},\tilde{l}'}^{(i)} - \mathbb{E}[\tilde{b}_{\tilde{k},\tilde{l}'}^{(i)}])^2]}{(W+1)\tilde{c}_{l,\tilde{k},\tilde{l}'}} \end{aligned} \quad (16)$$

respectively. We use the GA of (15) to approximate the update rule (13) by

$$\begin{aligned} q_{n,l}^{(i)}(b_{k,l'}) &= \mathbb{E}_{\tilde{l}_{n,l,k,l'}^{(i-1)}} \left[p \left(y_{n,l} \left| \frac{s_{n,l,k,l'} b_{k,l'}}{\sqrt{(W+1)\tilde{c}_{l,k,l'}}} + \tilde{l}_{n,l,k,l'}^{(i-1)} \right. \right) \right] \\ &\approx g \left(y_{n,l} - \frac{s_{n,l,k,l'} b_{k,l'}}{\sqrt{(W+1)\tilde{c}_{l,k,l'}}} - \tilde{\mu}_{n,l,k,l'}^{(i-1)}; \tilde{v}_{n,l,k,l'}^{(i-1)} + \sigma_n^2 \right), \end{aligned} \quad (18)$$

where $g(x; \sigma^2)$ denotes the pdf (1) for a zero-mean Gaussian random variable with variance σ^2 . The complexity of the BP receiver with GA (18) is linear in the row weight r , as well as in K and L .

IV. MAIN RESULTS

A. Density Evolution Analysis

The asymptotic properties of the BP receiver (12) are analyzed in this section. Let us define the equivalent channel between $b_{k,l'}$ and the corresponding output in iteration i , denoted by $b_{k,l'}^{(i)}$, as

$$p(b_{k,l'}^{(i)} | b_{k,l'}) = \overline{\int p^{(i)}(b_{k,l'} = b_{k,l'}^{(i)} | \mathcal{Y}, \mathbf{G}) p(\mathcal{Y} | \mathbf{G}, b_{k,l'}) d\mathcal{Y}}, \quad (19)$$

where the overline represents the expectation with respect to \mathbf{G} . The average BER and SIR can be calculated from the equivalent channel (19).

We consider five limits: the large-system limit, the dense limit $r \rightarrow \infty$, the continuum limit $L, W \rightarrow \infty$ with $\gamma = W/L$ kept constant, the infinite-iteration limit $i \rightarrow \infty$, and $\gamma \rightarrow 0$. We first present the main result in the first two limits, i.e. in the large-sparse-system limit where the dense limit $r \rightarrow \infty$ is taken *after* the large-system limit. The main result is that the equivalent channel (19) converges to the one for a scalar AWGN channel in the large-sparse-system limit. The remaining three limits will be investigated in the next section.

We first introduce the equivalent AWGN channel for iteration i ,

$$z_{k,l'}^{(i)} = b_{k,l'} + w_{k,l'}^{(i)}, \quad (20)$$

with $w_{k,l'} \sim \mathcal{N}(0, (\text{sir}_{l'}^{(i)})^{-1})$, in which $\text{sir}_{l'}^{(i)}$ will be defined shortly. Let $\langle b_{k,l'} \rangle_i$ denote the posterior mean estimator of $b_{k,l'}$ in iteration i ,

$$\langle b_{k,l'} \rangle_i = \sum_{b_{k,l'} = \pm 1} b_{k,l'} p(b_{k,l'} | z_{k,l'}^{(i)}), \quad (21)$$

where the posterior probability $p(b_{k,l'} | z_{k,l'}^{(i)})$ in iteration i is defined as

$$p(b_{k,l'} | z_{k,l'}^{(i)}) = \frac{p(z_{k,l'}^{(i)} | b_{k,l'}) p(b_{k,l'})}{p(z_{k,l'}^{(i)})}, \quad (22)$$

with

$$p(z_{k,l'}^{(i)}) = \sum_{b_{k,l'} = \pm 1} p(z_{k,l'}^{(i)} | b_{k,l'}) p(b_{k,l'}). \quad (23)$$

The MSE $\xi(\text{sir}_{l'}^{(i)})$ for the posterior mean estimator (21) in iteration i is given by

$$\xi(\text{sir}_{l'}^{(i)}) = \mathbb{E}[(b_{k,l'} - \langle b_{k,l'} \rangle_i)^2]. \quad (24)$$

Theorem 1: Suppose that (7) is picked up from the (r, L, W) -ensemble, presented in Example 3. Then, the equivalent channel (19) for the BP receiver in iteration i converges to the equivalent channel for the scalar AWGN channel (20) in the large-sparse-system limit:

$$p(b_{k,l'}^{(i)} | b_{k,l'}) \rightarrow \int p(b_{k,l'} = b_{k,l'}^{(i)} | z_{k,l'}^{(i)}) p(z_{k,l'}^{(i)} | b_{k,l'}) dz_{k,l'}^{(i)}. \quad (25)$$

In (25), the posterior probability $p(b_{k,l'} | z_{k,l'}^{(i)})$ is given by (22). The conditional pdf $p(z_{k,l'}^{(i)} | b_{k,l'})$ represents the scalar AWGN channel (20) in iteration i . In evaluating these expressions, the asymptotic SIR $\text{sir}_{l'}^{(i)}$ is given via the coupled equations

$$\text{sir}_{l'}^{(i)} = \frac{1}{W+1} \sum_{w=0}^W \frac{1}{\sigma_{(l'+w)_L}^2(i)}, \quad (26)$$

$$\sigma_l^2(i) = \sigma_n^2 + \frac{\beta_l}{W+1} \sum_{w=0}^W \xi(\text{sir}_{(l-w)_L}^{(i-1)}), \quad (27)$$

with $\text{sir}_{l'}^{(0)} = 0$ for all $l' \in \mathcal{L}$. In (27), $\beta_l = K/N_l$ is equal to β_{init} for $l = 0, \dots, W-1$ and to β for $l = W, \dots, L-1$, respectively.

Proof: See Appendix A. ■

The expressions (26) and (27) determine the evolution of the asymptotic equivalent channel (25) with respect to i . Thus, they are referred to as DE equations.

As is obvious from the proof of Theorem 1, the GA for the postulated interference (15) is exact in the large-sparse-system limit. Thus, we have the following result.

Theorem 2: Suppose that (7) is picked up from the (r, L, W) -ensemble, presented in Example 3. Then, the equivalent channel for the BP receiver with GA converges to the asymptotic equivalent channel for the true BP receiver, i.e. the right-hand side (RHS) of (25) in the large-sparse-system limit.

Proof: Repeat the proof of Theorem 1. ■

From Theorem 2, the performance of the BP receiver with GA is indistinguishable from that of the true BP receiver in the large-sparse-system limit. Thus, we hereafter focus on the true BP receiver.

We here investigate the performance of the BP receivers for finite L and W . It is proved that the asymptotic SIRs (26) monotonically converge toward a fixed-point of the DE equations (26) and (27) as $i \rightarrow \infty$.

Proposition 1: For all positions l' ,

$$\text{sir}_{l'}^{(0)} \leq \text{sir}_{l'}^{(1)} \leq \dots \leq \text{sir}_{l'}^{(\infty)}, \quad (28)$$

where $\{\text{sir}_{l'}^{(\infty)} : l' \in \mathcal{L}\}$ denotes a fixed-point of the DE equations (26) and (27).

Proof: See the proof of Lemma 1 in Section V. ■

It is shown that the BP receiver can achieve the same performance as that for the (soft) IO receiver if the fixed-point is unique.

Theorem 3: Suppose that (7) is picked up from the (r, L, W) -ensemble, presented in Example 3. If the fixed-point of the DE equations (26) and (27) is unique, the asymptotic SIR for the BP receiver converges to that for the (soft) IO receiver in the infinite-iteration limit $i \rightarrow \infty$ after taking the large-sparse-system limit.

Proof: We follow an argument based on a genie-aided BP receiver in [23] to prove Theorem 3. For a fixed number of iterations i , let $\mathcal{Y}_{k,l'}^{(i)}$ denote the set of the received signals $\{y_{n,l'}\}$ utilized in the BP detection of $b_{k,l'}$. The data symbols are classified into two groups: the data symbols $\mathcal{X}_{k,l'}^{(i)}$ that connect only to the function nodes in $\mathcal{Y}_{k,l'}^{(i)}$, and the remaining data symbols. The ACF property of the (r, L, W) ensemble implies that $\mathcal{X}_{k,l'}^{(i)}$ consists of the data symbols whose depth (distance from the root $b_{k,l'}$) is less than or equal to $2(i-1)$. Furthermore, $\mathcal{Y}_{k,l'}^{(i)}$ is composed of the function nodes that have depth less than $2i$. The BP detection of $b_{k,l'}$ with the number of iterations i is equivalent to the soft IO detection of $b_{k,l'}$ based on $\mathcal{Y}_{k,l'}^{(i)}$, whereas the soft IO detection of $b_{k,l'}$ is based on the entire received signals \mathcal{Y} . We use a genie-aided BP receiver to obtain an upper bound on the asymptotic SIR of the soft IO receiver. Let a genie inform the BP receiver about the data symbols not in $\mathcal{X}_{k,l'}^{(i)}$. Since information about the received signals not in $\mathcal{Y}_{k,l'}^{(i)}$ is passed only through the *known* data symbols with depth $2i$, using the information $\mathcal{Y} \setminus \mathcal{Y}_{k,l'}^{(i)}$ does not improve the performance of the genie-aided BP receiver. Thus, the soft IO receiver cannot outperform the genie-aided

BP receiver. In other words, the asymptotic SIR for the genie-aided BP receiver provides an upper bound on that for the soft IO receiver.

The performance of the genie-aided BP receiver can be evaluated in the large-sparse-system limit by repeating the proof of Theorem 1. The asymptotic SIR converges to (26), which are determined by the DE equations (26) and (27). The only difference is that the initial condition is not $\text{sir}_{l'}^{(0)} = 0$ but $\text{sir}_{l'}^{(0)} = \infty$, because the data symbols with depth $2i$ are known to the receiver. Let us take the infinite-iteration limit $i \rightarrow \infty$. Since we have assumed that the DE equations have the unique fixed-point, the solution to the DE equations converges to the unique fixed-point as $i \rightarrow \infty$, regardless of the initial condition. This observation implies that the performance of the genie-aided BP receiver coincides with that of the BP receiver as $i \rightarrow \infty$ after taking the large-sparse-system limit. Since the performance of the soft IO receiver is sandwiched between the performance of the two BP receivers, the BP receiver can achieve the same performance as that for the soft IO receiver. ■

B. Threshold Analysis

We have so far considered the two limits: the large-system limit and the dense limit. In this section, the remaining limits are investigated. We start with the definition of the BP threshold.

Definition 1 (BP Threshold): Let $\{\text{sir}_{l'}^{(\text{opt})}\}$ denote the fixed-point of the DE equations (26) and (27) that has the largest SIR at the middle point $l'/L = 1/2$ among all possible fixed-points. The BP threshold is defined as the supremum of β_{th} such that $L^{-1} \sum_{l' \in \mathcal{L}} |\text{sir}_{l'}^{(i)} - \text{sir}_{l'}^{(\text{opt})}|$ converges to zero for all $\beta \in (0, \beta_{\text{th}})$.

Let us postulate that the DE equations (26) and (27) for the uncoupled case $W = 0$ have multiple fixed-points. For the SC-SCDMA system with $W > 0$, reliable information about the data symbols should propagate toward the middle point $l'/L = 1/2$. Thus, the asymptotic SIR at the middle point should be worst among those for all positions. Furthermore, the SIR $\text{sir}_{L/2}^{(\text{opt})}$ at the middle point is close to $1/\sigma_n^2$ for high SNR when β is below the BP threshold, as shown in Section VI, so that the SIRs $\{\text{sir}_{l'}^{(\text{opt})}\}$ are close to $1/\sigma_n^2$ at all positions. This implies that the BP threshold corresponds to a boundary between the interference-limited region and the non-limited region for the BP receivers. The BP receivers can mitigate the MAI well when β is below the BP threshold.

If the DE equations (26) and (27) for $W > 0$ have the unique fixed-point $\{\text{sir}_{l'}^{(\text{opt})}\}$, the asymptotic SIRs converge to $\{\text{sir}_{l'}^{(\text{opt})}\}$ as $i \rightarrow \infty$. Otherwise, the asymptotic SIRs are expected to be trapped in the other fixed-point, as noted in Section V. Thus, the BP threshold should be equal to the supremum of β_{th} such that the DE equations (26) and (27) have the unique fixed-point for all system loads $\beta \in (0, \beta_{\text{th}})$.

We focus on the BP threshold for the SC system in the limit $L, W \rightarrow \infty$ with $\gamma = W/L \rightarrow 0$, since analytical evaluation of the BP threshold for finite L and $W > 0$ is intractable. In order to distinguish the BP threshold for the SC system from that for the uncoupled system, the one for the uncoupled

system $W = 0$ is denoted by β_{BP} . On the other hand, the BP threshold for the SC system in the limit $L, W \rightarrow \infty$ with $\gamma = W/L \rightarrow 0$ is written as $\beta_{BP}^{(SC)}$.

Before evaluating the BP threshold $\beta_{BP}^{(SC)}$ for the SC-SCDMA system, we shall review the performance assessment of the soft IO receiver for the uncoupled dense CDMA system based on the non-rigorous replica method [10], [12], and define the IO threshold.

Proposition 2 (Tanaka 2002): The asymptotic SIR of the soft IO receiver for the uncoupled dense BPSK-input CDMA system with system load β converges to s in the large-system limit, in which s is a solution to the following fixed-point equation,

$$\frac{1}{s} = \sigma_n^2 + \beta \xi(s), \quad (29)$$

where $\xi(s)$ denotes the MSE for the posterior mean estimator of the BPSK data symbol transmitted through the scalar AWGN channel with SNR s . If the fixed-point equation has multiple solutions, the solution s is selected to minimize the free energy

$$F(s) = \beta C(s) + \frac{1}{2} [\sigma_n^2 s - \ln(\sigma_n^2 s) - 1], \quad (30)$$

where $C(s)$ denotes the input-output mutual information in nats for the BPSK-input scalar AWGN channel with SNR s .

The fixed-points of the DE equations (26) and (27) for the uncoupled SCDMA system $W = 0$ coincide with the solutions to the fixed-point equation (29). When the fixed-point equation (29) has multiple solutions, there is a difference in performance between the BP and IO receivers for the uncoupled case. The IO receiver can achieve the largest solution to (29) if it is the global minimum of the free energy (30), whereas the BP receivers cannot.

It is straightforward to find that the solution s to the fixed-point equation (29) corresponds to a stationary point of the free energy (30), with a general relationship proved in [48] between the mutual information $C(s)$ and the MSE $\xi(s)$ for the scalar AWGN channel

$$\frac{dC}{ds}(s) = \frac{1}{2} \xi(s). \quad (31)$$

Korada and Montanari [49] proved that the minimum of the free energy (30) over s is equal to the sum capacity in nats for the uncoupled dense CDMA system with BPSK inputs in the large-system limit. Unfortunately, it is still open whether or not the asymptotic SIR for the soft IO receiver coincides with the solution s minimizing the free energy (30) when the fixed-point equation (29) has multiple solutions, although the non-rigorous replica analysis [10], [12] suggests so.

The fixed-point equation (29) has the unique solution for all system loads in the low-to-moderate SNR regime. On the other hand, it has multiple solutions for high system loads³ in the high SNR regime. In other words, the free energy (30) is bistable for high system loads, as shown in Fig. 1. The latter situation is the target of spatial coupling.

Only the free energy (30) at the solutions to (29) is used in Proposition 2. Consequently, one can apply any change

of variables as long as it maps the global stable solution of the original free energy to that of the obtained one. We use this ambiguity to derive another expression of the free energy that is suitable for understanding the BP threshold for the SC-SCDMA system. Let us consider the free energy $\tilde{F}(s)$ obtained by substituting (29) into s in the second term of (30),

$$\begin{aligned} \tilde{F}(s) &= \beta C(s) + \frac{1}{2} \left[\frac{\sigma_n^2}{\sigma_n^2 + \beta \xi(s)} - \ln \frac{\sigma_n^2}{\sigma_n^2 + \beta \xi(s)} - 1 \right] \\ &= \beta C(s) + \frac{1}{2} \left[\ln \frac{\sigma_n^2 + \beta \xi(s)}{\sigma_n^2} - \beta s \xi(s) \right]. \end{aligned} \quad (32)$$

In the derivation of the last expression, we have used (29) again. The statement of Proposition 2 would be unchanged even if the free energy (32) were used instead of (30).

Remark 1: The shape of the free energy (32) as a function of s is qualitatively the same as that of the original one (30). In fact, calculating the stationarity condition for (32) yields

$$\tilde{F}'(s) = \frac{\beta \xi'(s)}{2} \left[\frac{1}{\sigma_n^2 + \beta \xi(s)} - s \right] = 0, \quad (33)$$

where we have used (31). Since the MSE $\xi(s)$ is a monotonically decreasing function of SNR s , the stationarity condition (33) reduces to the original one (29). The values of the free energy (32) at the stationary points coincide with those of the original one (30) at the same stationary points. Furthermore, any two adjacent stationary points in the free energy are connected by a monotonic curve. These observations imply that the metastable, unstable, and global stable solutions to the free energy (32) are equal to the corresponding solutions of the original one (30), respectively.

We shall present the definition of the IO threshold for the uncoupled CDMA system.

Definition 2 (IO Threshold): The IO threshold β_{IO} for the uncoupled CDMA system is defined as the supremum of β_{th} such that the asymptotic SIR for the IO receiver is equal to the largest solution of the free energy (30) or (32) for all $\beta \in (0, \beta_{th})$.

Proposition 2 implies that the IO threshold β_{IO} is equal to the system load β such that the free energy (30) or (32) has two global minima. It is obvious that the IO threshold β_{IO} is larger than the conventional BP threshold β_{BP} . The IO threshold corresponds to a boundary between the interference-limited region and the non-limited region for the IO receiver. The IO receiver can mitigate the MAI well when β is below the IO threshold.

We move on to the evaluation of the BP threshold for the SC-SCDMA system. The following result implies that the BP threshold can be improved up to the IO threshold by spatial coupling.

Theorem 4: Let $\beta_{init} = 0$ and take the continuum limit $L, W \rightarrow \infty$ with $\gamma = W/L$ kept constant, $i \rightarrow \infty$, and finally $\gamma \rightarrow 0$. Then,

$$\beta_{IO} \leq \beta_{BP}^{(SC)}. \quad (34)$$

Proof: We use the two functions $\psi(v) = -\xi(v)$ and $\varphi(u) = 1/(\sigma_n^2 - u)$ to define a potential energy function as

$$V(u) = vu - \int \beta \psi(v) dv - \int \varphi(u) du, \quad (35)$$

³This is the definition of the term ‘‘high system load’’ in this paper.

with $v = \psi^{-1}(u/\beta)$. In (35), the integrals denote indefinite integrals. Let $\tilde{\beta}_{\text{BP}}^{(\text{SC})}$ denote the potential threshold that is defined as β such that the potential (35) has two global minima. In Section V we will prove $\tilde{\beta}_{\text{BP}}^{(\text{SC})} \leq \beta_{\text{BP}}^{(\text{SC})}$. Thus, it is sufficient to show $\tilde{\beta}_{\text{BP}}^{(\text{SC})} = \beta_{\text{IO}}$.

Calculating the RHS of (35) with (31) and $u = \beta\psi(v)$, we obtain

$$V(u) = -\beta v \xi(v) + 2\beta C(v) + \ln(\sigma_n^2 + \beta \xi(v)) + A, \quad (36)$$

with any constant A . Setting $A = -\ln \sigma_n^2$ yields $V(u) = 2\tilde{F}(\psi^{-1}(u/\beta))$, given by (32). Since the transformation of variables $v = \psi^{-1}(u/\beta)$ does not change the qualitative shape of the free energy (32), from the definition of the IO threshold we find $\tilde{\beta}_{\text{BP}}^{(\text{SC})} = \beta_{\text{IO}}$. ■

As shown in Section V, the DE equations (26) and (27) have the unique fixed-point in the limit $W, L \rightarrow \infty$ with $\gamma \rightarrow 0$ if β is smaller than the IO threshold β_{IO} . From Theorem 3, the BP receiver is optimal in the limit $W, L \rightarrow \infty$ with $\gamma \rightarrow 0$ for $\beta < \beta_{\text{IO}}$ if the limit $W, L \rightarrow \infty$ with $\gamma = W/L$ fixed commutes with the infinite-iteration limit $i \rightarrow \infty$ in Theorem 3, whereas Theorem 3 was proved in the limit $i \rightarrow \infty$ for finite L and W .

Remark 2: We shall conjecture the position of the BP threshold $\beta_{\text{BP}}^{(\text{SC})}$ for the SC-SCDMA system. The non-rigorous replica analysis presented in [29] implies that the IO threshold $\beta_{\text{IO}}^{(\text{SC})}$ for the SC-CDMA system converges to the conventional IO threshold β_{IO} from above in the limit $L, W \rightarrow \infty$ with $\gamma \rightarrow 0$. Since the BP threshold $\beta_{\text{BP}}^{(\text{SC})}$ is bounded from above by $\beta_{\text{IO}}^{(\text{SC})}$, we obtain $\beta_{\text{BP}}^{(\text{SC})} \leq \beta_{\text{IO}}$ in the limit $L, W \rightarrow \infty$ with $\gamma \rightarrow 0$. Combining this upper bound and Theorem 4, we can conclude

$$\beta_{\text{BP}}^{(\text{SC})} = \beta_{\text{IO}}, \quad (37)$$

if the replica analysis provides a correct result. Thus, we hereafter refer to the potential threshold $\tilde{\beta}_{\text{BP}}^{(\text{SC})}$ as the BP threshold for the SC-SCDMA system.

The convergence of $\beta_{\text{IO}}^{(\text{SC})}$ to β_{IO} implies that spatial coupling never improves the performance of IO detection. In other words, spatial coupling should be regarded as a method for improving the performance of iterative detection. Unfortunately, we can provide no rigorous proof for the convergence, which may be intuitively understood as follows: The reason why $\beta_{\text{IO}}^{(\text{SC})}$ is above β_{IO} is due to the rate loss, which vanishes in the limit $L, W \rightarrow \infty$ with $\gamma \rightarrow 0$.

V. PHENOMENOLOGICAL STUDY ON SPATIAL COUPLING

A. Continuum Limit

1) *Density-Evolution Equations:* We shall present the proof of Theorem 4 in a general setting. We assume that two functions $\varphi(u)$ and $\psi(v)$ are bounded, strictly increasing, twice continuously differentiable. Let $\mathcal{D} \subset \mathbb{R}$ and $\tilde{\mathcal{D}} \subset \mathbb{R}$ denote the images of φ and ψ , respectively. We assume that \mathcal{D} and $\tilde{\mathcal{D}}$ are bounded, and that the supremum u_{\max} of $\tilde{\mathcal{D}}$ is equal to $u_{\max} = 0$, without loss of generality. Let $(v_l(i), u_l(i)) \in \mathcal{D} \times \tilde{\mathcal{D}}$ denote the state in iteration $i \geq 0$ at position $l \in \mathcal{L} = \{0, \dots, L-1\}$ of an SC system with the

number of subsystems L and coupling width W , governed by the following DE equations

$$v_l(i) = \frac{1}{W+1} \sum_{w=0}^W \varphi(u_{(l+w)_L}(i)), \quad (38)$$

$$u_l(i) = \frac{\beta_l}{W+1} \sum_{w=0}^W \psi(v_{(l-w)_L}(i-1)), \quad (39)$$

with the initial condition $v_l(0) = v_{\min} \equiv \inf \mathcal{D}$. In (39), the parameter $\beta_l \geq 0$ is given by

$$\beta_l = \begin{cases} 0 & l \in \{0, \dots, W-1\} \\ \beta & l \in \{W, \dots, L-1\}. \end{cases} \quad (40)$$

The DE equations (38) and (39) include (26) and (27) for the SC-SCDMA system as a special case, which can be confirmed by letting $v_l(i) = \text{sir}_l^{(i)}$, $u_l(i) = \sigma_n^2 - \sigma_l^2(i) \leq 0$, $\varphi(u) = 1/(\sigma_n^2 - u)$, and $\psi(v) = -\xi(v)$.

From (40) the DE equations (38) and (39) can be represented as

$$v_l(i) = \frac{1}{W+1} \sum_{w=0}^W \varphi(u_{l+w}(i)) \quad l \in \{0, \dots, L-1\}, \quad (41)$$

$$u_l(i) = \frac{\beta}{W+1} \sum_{w=0}^W \psi(v_{l-w}(i-1)) \quad l \in \{W, \dots, L-1\}, \quad (42)$$

with $u_l(i) = 0$ for $l \notin \{W, \dots, L-1\}$. Note that the boundaries are fixed to the supremum $u_{\max} = 0$ of the set $\tilde{\mathcal{D}}$. The monotonicity $\varphi'(u) > 0$ implies that $v_{\max} = \varphi(u_{\max})$ is also the supremum of \mathcal{D} .

Let v_r denote the largest solution to the fixed-point equation $v = \varphi(\beta\psi(v))$ for the uncoupled case. The solution (v_r, u_r) satisfies the following fixed-point equations:

$$v_r = \varphi(u_r), \quad u_r = \beta\psi(v_r). \quad (43)$$

We assume that (v_r, u_r) is a stable fixed-point for the DE equations (41) and (42) in the uncoupled case $W = 0$.

We first prove that the DE equations (41) and (42) are convergent as $i \rightarrow \infty$.

Lemma 1: For any $l \in \mathcal{L}$ and i ,

$$v_l(i) \leq v_l(i+1), \quad u_l(i) \leq u_l(i+1). \quad (44)$$

Proof: We follow [35] to prove the statement by induction. For $i = 0$ the statement $v_l(0) \leq v_l(1)$ holds for any l because of $v_l(0) = v_{\min}$. Assume $v_l(i-1) \leq v_l(i)$ for all x . From (42), we obtain

$$\begin{aligned} u_l(i+1) - u_l(i) &= \frac{\beta}{W+1} \sum_{w=0}^W \{\psi(v_{l-w}(i)) - \psi(v_{l-w}(i-1))\} \geq 0, \end{aligned} \quad (45)$$

for all $l \in \{W, \dots, L-1\}$. In the derivation of the inequality, we have used the assumption $v_l(i-1) \leq v_l(i)$ and $\psi'(v) > 0$. Combining this observation and the boundary condition $u_l(i) = u_{\max}$ for any i and $l \notin \{W, \dots, L-1\}$, we obtain $u_l(i) \leq u_l(i+1)$ for any $l \in \mathcal{L}$. Repeating the same argument for (41), we find $v_l(i) \leq v_l(i+1)$ for any $l \in \mathcal{L}$. By induction, the statement holds for any i . ■

We take three limits to analyze the DE equations (41) and (42): In a first limit called *continuum limit*, L and W tend to infinity while the ratio $\gamma = W/L$ is kept constant. A second limit is the infinite-iteration limit $i \rightarrow \infty$. In the last limit, γ tends to zero. The goal of Section V-A is to prove that the state governed by the DE equations converges to a stationary solution of a temporally-continuous and spatially-continuous partial differential equation in the limits above. The proof strategy is as follows: We first take the continuum limit to reduce the DE equations (41) and (42) to discrete-time and spatially-continuous integral systems. Subsequently, we approximate the integral systems by a continuous-time partial differential equation as $\gamma \rightarrow 0$ after taking $i \rightarrow \infty$, whereas Donoho et al. [35] analyzed the integral systems directly. The main theorem in Section V-A can be rigorously proved by deriving the partial differential equation via the integral systems. Furthermore, the partial differential equation provides an intuitive understanding of spatial coupling, as shown in Section V-B.

2) *Integral Systems*: We define two spatially-continuous state functions $v_\gamma(x, i)$ and $u_\gamma(x, i)$ as

$$v_\gamma(x, i) = \mathfrak{F}[u_\gamma(\cdot, i); \varphi](x), \quad |x| \leq 1, \quad (46)$$

$$u_\gamma(x, i) = \begin{cases} \beta \mathfrak{F}[v_\gamma(\cdot, i-1); \psi](x) & |x| < 1 - \gamma \\ u_{\max} & |x| \geq 1 - \gamma, \end{cases} \quad (47)$$

with

$$\mathfrak{F}[u; \varphi](x) = \frac{1}{2\gamma} \int_{-\gamma}^{\gamma} \varphi(u(x + \omega)) d\omega. \quad (48)$$

We impose the initial condition $v_\gamma(x, 0) = v_{\min}$ for $|x| \leq 1$.

Let $\mathcal{C}_{1-2\gamma}^2$ denote the space of continuous even functions on $[-1, 1]$ that are twice continuously differentiable on $(-1, 1) - \{\pm(1 - 2\gamma)\}$. The function $v_\gamma(x, i)$ is shown to be contained in the space $\mathcal{C}_{1-2\gamma}^2$ for any i .

Lemma 2:

1) For any x, i , and any $\gamma > 0$,

$$v_\gamma(x, i) \leq v_\gamma(x, i+1), \quad u_\gamma(x, i) \leq u_\gamma(x, i+1). \quad (49)$$

2) For any i , $u_\gamma(x, i)$ is an even function and continuous on $\mathbb{R} - \{\pm(1 - \gamma)\}$. Furthermore, $v_\gamma(x, i) \in \mathcal{C}_{1-2\gamma}^2$ for any i .

3) For any i and $\gamma > 0$,

$$\begin{aligned} \lim_{W=\gamma L \rightarrow \infty} \frac{1}{L} \sum_{l \in \mathcal{L}} \left| v_l(i) - v_\gamma \left(\frac{2l}{L} - 1, i \right) \right| &= 0, \\ \lim_{W=\gamma L \rightarrow \infty} \frac{1}{L} \sum_{l \in \mathcal{L}} \left| u_l(i) - u_\gamma \left(\frac{2l}{L} - 1 - \gamma, i \right) \right| &= 0. \end{aligned} \quad (50)$$

Proof: The first property is proved by repeating the proof of Lemma 1. Thus, we shall prove the second property. The symmetry of $v_\gamma(x, i)$ and $u_\gamma(x, i)$ follows from the symmetries of the initial condition $v_\gamma(x, 0) = v_{\min}$ and of the integral systems (46) and (47). It is straightforward to observe

that, for any even function $u(x)$, the function $\mathfrak{F}[u; \varphi](x)$ is also an even function. Indeed, one has

$$\begin{aligned} \mathfrak{F}[u; \varphi](-x) &= \frac{1}{2\gamma} \int_{-\gamma}^{\gamma} \varphi(u(-x + \omega)) d\omega \\ &= \frac{1}{2\gamma} \int_{-\gamma}^{\gamma} \varphi(u(-x - \omega)) d\omega \\ &= \frac{1}{2\gamma} \int_{-\gamma}^{\gamma} \varphi(u(x + \omega)) d\omega = \mathfrak{F}[u; \varphi](x). \end{aligned} \quad (52)$$

Thus, the integral systems (46) and (47) with the even initial function $v_\gamma(x, 0) = v_{\min}$ define even functions $v_\gamma(x, i)$ and $u_\gamma(x, i)$ for any i .

Let us show the statement on continuity. Expression (46) can be represented as

$$v_\gamma(x, i) = \frac{1}{2\gamma} \int_{x-\gamma}^{x+\gamma} \varphi(u_\gamma(\omega, i)) d\omega, \quad |x| \leq 1. \quad (53)$$

Since the initial function $v_\gamma(x, 0) = v_{\min}$ is measurable, the integral systems (46) and (47) with the bounded functions φ and ψ define measurable functions $v_\gamma(x, i)$ and $u_\gamma(x, i)$ for any i . This observation and the boundedness of φ and ψ imply that the integrand in (53) is Lebesgue-integrable. Thus, $v_\gamma(x, i)$ is (absolutely) continuous [50] on $[-1, 1]$ for any i . Repeating the same argument for (47), we find that $u_\gamma(x, i)$ is continuous for $|x| < 1 - \gamma$. Combining this observation and the boundary condition $u_\gamma(x, i) = u_{\max}$ for $|x| \geq 1 - \gamma$, the function $u_\gamma(x, i)$ is continuous on $\mathbb{R} - \{\pm(1 - \gamma)\}$.

The statement on differentiability follows from (53). When the integrand in (53) is continuous at $\omega = x \pm \gamma$, from the fundamental theorem of calculus [51], the derivative of (53) exists and is given by

$$\frac{dv_\gamma}{dx}(x, i) = \frac{\varphi(u_\gamma(x + \gamma, i)) - \varphi(u_\gamma(x - \gamma, i))}{2\gamma}. \quad (54)$$

Since $u_\gamma(x, i)$ is continuous with the exception of $x = \pm(1 - \gamma)$, $v_\gamma(x, i)$ is continuously differentiable on $(-1, 1) - \{\pm(1 - 2\gamma)\}$. Repeating the same argument for $u_\gamma(x, i)$, we find that $u_\gamma(x, i)$ is continuously differentiable with the exception of the discontinuous points $x = \pm(1 - \gamma)$. The function $v_\gamma(x, i)$ is twice continuously differentiable when the RHS of (53) is continuously differentiable. Thus, $v_\gamma(x, i)$ is twice continuously differentiable on $(-1, 1) - \{\pm(1 - 2\gamma)\}$.

The last property holds from the definition of the Riemann integral. See [35] for a formal proof of the last property by induction. We here present a sketch of the proof. Assume that (50) holds for some i . From (42) and (47), calculating the difference $|u_l(i+1) - u_\gamma(x_l - \gamma, i+1)|$ for $x_l = (2l/L) - 1$ yields

$$\begin{aligned} &|u_l(i+1) - u_\gamma(x_l - \gamma, i+1)| \\ &< \frac{1}{W+1} \sum_{w=0}^W |\psi(v_l(i)) - \psi(v_\gamma(x_{l-w}, i))| \\ &+ \left| \frac{1}{W+1} \sum_{w=0}^W \psi(v_\gamma(x_{l-w}, i)) \right. \\ &\quad \left. - \frac{1}{2\gamma} \int_{-\gamma}^{\gamma} \psi(v_\gamma(x_l - \gamma + \omega, i)) d\omega \right|. \end{aligned} \quad (55)$$

Taking the sum $L^{-1} \sum_{l \in \mathcal{L}}$, letting $\omega = -(2w/L) + \gamma$, and considering the continuum limit, it is possible to show that the first term tends to zero from the assumption (50). Furthermore, the second term is also proved to converge to zero from the definition of the Riemann integral. Repeating the same argument for (41) and (46) results in the last property of Lemma 2. ■

From the first property in Lemma 2, it is guaranteed that the state $(v_\gamma(x, i), u_\gamma(x, i))$ of the integral systems (46) and (47) converges a stationary solution $(v_\gamma(x), u_\gamma(x))$ as $i \rightarrow \infty$. Since the integrands in (46) and (47) are bounded, we can use the dominated convergence theorem [50] to exchange the order of the limit $i \rightarrow \infty$ and the integrals. Thus, any stationary solution $(v_\gamma(x), u_\gamma(x))$ satisfies the fixed-point equations

$$v_\gamma(x) = \mathfrak{F}[u_\gamma(\cdot); \varphi](x), \quad |x| \leq 1, \quad (56)$$

$$u_\gamma(x) = \begin{cases} \beta \mathfrak{F}[v_\gamma(\cdot); \psi](x) & |x| < 1 - \gamma \\ u_{\max} & |x| \geq 1 - \gamma, \end{cases} \quad (57)$$

with \mathfrak{F} defined in (48). Although differentiability for stationary solutions is non-trivial in general, we can prove that any stationary solution $(v_\gamma(x), u_\gamma(x))$ has the same differentiability as $(v_\gamma(x, i), u_\gamma(x, i))$.

Lemma 3: Suppose that $v_\gamma(x)$ is any stationary solution to the fixed-point equations (56) and (57). Then, $v_\gamma(x) \in \mathcal{C}_{1-2\gamma}^2$.

Proof: Repeat the proof of the second property in Lemma 2, by using the fact that the sequence of measurable functions converges to a measurable function. ■

3) *Differential Systems:* We study stationary solutions to the fixed-point equations (56) and (57) in the limit $\gamma \rightarrow 0$. It is done by introducing a continuous-time system with a state function $u(x, t)$ for $x \in [-1, 1]$ at time $t \geq 0$, whose time evolution is governed by a partial differential equation. The continuous-time system is to be constructed so that any stable solution to the fixed-point equations (56) and (57) is characterized in the limit $\gamma \rightarrow 0$ by a stationary solution to the partial differential equation. Intuitively, one may regard the derivative $\partial u(x, t)/\partial t$ as an approximation of the difference $u_\gamma(x, t+1) - u_\gamma(x, t)$.

Let us define a potential function $V(u)$ as

$$V(u) = -D(\psi^{-1}(u/\beta)\|u), \quad (58)$$

where $D(v\|u)$ similar to the divergence⁴ in information geometry [52] is given by

$$D(v\|u) = \int \beta \psi(v) dv + \int \varphi(u) du - vu. \quad (59)$$

The integrals in (59) denote indefinite integrals, so that the first and second terms in (59) are functions of v and u , respectively. Furthermore, we define a differential operator \mathcal{L} as

$$\mathcal{L}[u](x) = \frac{B'(u(x))}{2} \left(\frac{\partial u}{\partial x}(x) \right)^2 + B(u(x)) \frac{\partial^2 u}{\partial x^2}(x), \quad (60)$$

for a twice continuously differential function $u(x)$ on $[-1, 1]$, with

$$B(u) = \frac{1}{3} \varphi'(u) > 0. \quad (61)$$

⁴The indefinite integrals of φ and $\beta\psi$ are connected to each other via the Legendre transform in information geometry, whereas the two functions are independent functions in this paper.

Then, the partial differential equation that governs $u(x, t)$ is defined as

$$\frac{\partial u}{\partial t} = A(u(x, t)) \{-V'(u(x, t)) + \gamma^2 \mathcal{L}[u(\cdot, t)](x)\}, \quad (62)$$

with

$$A(u) = \beta \psi' \left(\psi^{-1} \left(\frac{u}{\beta} \right) \right) > 0. \quad (63)$$

We impose the boundary condition $u(\pm 1, t) = u_{\max}$ and the initial condition $u(x, 0) = \beta \psi(v_{\text{init}}(x))$. In the initial condition, $v_{\text{init}}(x)$ is a twice continuously differentiable function that satisfies $|v_{\text{init}}(x) - v_\gamma(x, \infty)| < \epsilon_{\text{init}}$ for any $\epsilon_{\text{init}} > 0$, with $v_\gamma(x, \infty)$ denoting the fixed-point of the integral systems (46) and (47) as $i \rightarrow \infty$. We note that such a function $v_{\text{init}}(x)$ exists from Lemma 3.

Lemma 4: For any $\epsilon > 0$ and $x \in [-1, 1]$, there exist some $t_0 > 0$ and stationary solution $u(x)$ such that

$$|u(x, t) - u(x)| < \epsilon, \quad (64)$$

for all $t \geq t_0$ and $\gamma > 0$.

Proof: See Appendix B for a sketch of the proof. ■

The goal of Section V-A is to prove the following theorem.

Theorem 5: Let $\tilde{v}(x) = \lim_{t \rightarrow \infty} \psi^{-1}(u(x, t)/\beta)$. Then,

$$\lim_{\gamma \rightarrow 0} \lim_{i \rightarrow \infty} \lim_{W=\gamma L \rightarrow \infty} \frac{1}{L} \sum_{l \in \mathcal{L}} \left| v_l(i) - \tilde{v} \left(\frac{2l}{L} - 1 \right) \right| = 0. \quad (65)$$

The potential (58) was originally defined in [30]. The contribution of this paper is to provide a systematic derivation of the potential via the approximation of the DE equations (41) and (42) by the partial differential equation (62).

Theorem 5 implies that the analysis of fixed-points to the DE equations (41) and (42) reduces to that of the structure of stationary solutions to the partial differential equation (62). The analysis will be presented in the next section to prove Theorem 4.

4) *Proof of Theorem 5:* The proof strategy of Theorem 5 is as follows: The relationship between the DE equations and the integral systems has been established in Lemma 2. Thus, we need to assess the relationship between the stationary solution $u(x)$ of the differential system (62) as $t \rightarrow \infty$ and that of the integral systems (46) and (47) as $i \rightarrow \infty$. In order to show that the difference between the two stationary solutions is negligibly small for sufficiently small γ , we use the two properties of the differential system: One property is the asymptotic stability of the differential system shown in Lemma 4. This implies that there exists some time $t_0 > 0$ such that the difference between the stationary solution $u(x)$ and the state $u(x, t_0)$ at time $t = t_0$ is negligibly small. The other property is that the state of the differential system moves very slowly for sufficiently small γ , since the differential system is an approximation of the integral systems as $\gamma \rightarrow 0$, and since the initial state of the differential system is very close to the fixed-point solution of the integral systems. This property implies a negligibly small change of the state for the differential system as long as finite time-evolution is considered. Combining the two properties yields Theorem 5.

We first prove the latter property. Let $v_\gamma(x) = \mathfrak{G}[v_\gamma(\cdot)](x)$ denote a single fixed-point equation for $v_\gamma(x)$ obtained by eliminating $u_\gamma(x)$ from the fixed-point equations (56) and (57). In order to evaluate the operator \mathfrak{G} , we define a continuous-time differential system as

$$\frac{\partial \tilde{v}}{\partial t} = -\tilde{v}(x, t) + \tilde{\mathfrak{G}}[\tilde{v}(\cdot, t)](x), \quad (66)$$

for $x \in [-1, 1]$. In (66), the operator $\tilde{\mathfrak{G}}$ is given by

$$\tilde{\mathfrak{G}}[\tilde{v}(\cdot, t)](x) = \varphi(\beta\psi(\tilde{v}(x, t))) + \gamma^2 \mathfrak{L}[\beta\psi(\tilde{v}(\cdot, t))](x), \quad (67)$$

with \mathfrak{L} defined in (60). We impose the boundary condition $\tilde{v}(\pm 1, t) = v_{\max}$ for any t and the initial condition $\tilde{v}(x, 0) = v_{\text{init}}(x)$, defined below (63).

We first confirm that the system (66) is equivalent to the partial differential equation (62) under the change of variables $u = \beta\psi(\tilde{v})$. This property and Lemma 4 imply that the differential system (66) is convergent as $t \rightarrow \infty$ for any $\gamma > 0$. The coefficient $A(u)$ in (62) is due to the chain rule $\partial u / \partial t = A(u) \partial \tilde{v} / \partial t$. Let us show that $\tilde{v} - \varphi(\beta\psi(\tilde{v}))$ corresponds to the derivative of the potential (58) under the change of variables. By definition,

$$\begin{aligned} \int \{\tilde{v} - \varphi(\beta\psi(\tilde{v}))\} du &= \int \{\tilde{v} - \varphi(\beta\psi(\tilde{v}))\} \beta\psi'(\tilde{v}) d\tilde{v} \\ &= -D(\tilde{v} \parallel \beta\psi(\tilde{v})), \end{aligned} \quad (68)$$

which is equal to $V(u)$, because of $\tilde{v} = \psi^{-1}(u/\beta)$. Thus, the partial differential equation (66) is equivalent to (62).

The differential system (66) is obtained by Taylor-expanding the RHSs of (46) and (47) with respect to γ around $\gamma = 0$ up to the second order for the bulk region $\mathcal{X} = (-1 - 2\gamma, 1 - 2\gamma)$.

Proposition 3: Suppose that $v(x)$ is any twice continuously differentiable function on $[-1, 1]$. For any $\epsilon > 0$, there exists some $\gamma_0 > 0$ such that

$$\int_{-1}^1 |\mathfrak{G}[v](x) - \tilde{\mathfrak{G}}[v](x)| dx < \epsilon, \quad (69)$$

for all $\gamma \in (0, \gamma_0)$.

Proof: Decomposing the integral (69) into two parts, we obtain

$$\begin{aligned} &\int_{-1}^1 |\mathfrak{G}[v](x) - \tilde{\mathfrak{G}}[v](x)| dx \\ &= \int_{\mathcal{X}} |\mathfrak{G}[v](x) - \tilde{\mathfrak{G}}[v](x)| dx + \int_{\bar{\mathcal{X}}} |\mathfrak{G}[v](x) - \tilde{\mathfrak{G}}[v](x)| dx, \end{aligned} \quad (70)$$

where $\bar{\mathcal{X}} = [-1, -(1 - 2\gamma)] \cup [1 - 2\gamma, 1]$ denotes the boundary region. We first upper-bound the second term. The second property of Lemma 2 implies that $\mathfrak{G}[v](x)$ is bounded on $[-1, 1]$ for given $v(x)$. Furthermore, from Lemma 4 we find that $\tilde{\mathfrak{G}}[v](x)$ is also bounded. Thus, the second term on the RHS of (70) is bounded from above by

$$\begin{aligned} &\int_{\bar{\mathcal{X}}} |\mathfrak{G}[v](x) - \tilde{\mathfrak{G}}[v](x)| dx \\ &< 4\gamma \left(\sup_{x \in \bar{\mathcal{X}}} |\mathfrak{G}[v](x)| + \sup_{x \in \bar{\mathcal{X}}} |\tilde{\mathfrak{G}}[v](x)| \right), \end{aligned} \quad (71)$$

which tends to zero as $\gamma \rightarrow 0$.

We next prove that the integrand $|\mathfrak{G}[v](x) - \tilde{\mathfrak{G}}[v](x)|$ in the first term of (70) tends to zero as $\gamma \rightarrow 0$ for $x \in \mathcal{X}$ in the bulk region. This will complete the proof of Proposition 3 because of the following argument: Since $|\mathfrak{G}[v](x) - \tilde{\mathfrak{G}}[v](x)|$ is bounded on \mathcal{X} for given $v(x)$, from the dominated convergence theorem we can exchange the order of the limit $\gamma \rightarrow 0$ and the integral $\int_{\mathcal{X}} dx$. These observations imply that the first term on the RHS of (70) tends to zero as $\gamma \rightarrow 0$. Thus, Proposition 3 holds.

Let us prove that $|\mathfrak{G}[v](x) - \tilde{\mathfrak{G}}[v](x)|$ tends to zero as $\gamma \rightarrow 0$ for $x \in \mathcal{X}$. Since $v(x)$ is twice continuously differentiable, we expand the integrand $\psi(v(x + \omega))$ in $\mathfrak{F}[v; \psi](x)$ given by (48) with respect to ω up to the second order to obtain

$$\mathfrak{F}[v; \psi](x) = \left(1 + \frac{\gamma^2}{6} \frac{d^2}{dx^2}\right) \psi(v(x)) + o(\gamma^2), \quad (72)$$

for $x \in \mathcal{X}$.

We next expand (46) for the bulk region $x \in \mathcal{X}$ to derive

$$\mathfrak{G}[v](x) = \left(1 + \frac{\gamma^2}{6} \frac{d^2}{dx^2}\right) \varphi(\beta\mathfrak{F}[v; \psi](x)) + o(\gamma^2), \quad (73)$$

for $x \in \mathcal{X}$. Substituting (72) into (73) and expanding the obtained expression with respect to γ , we arrive at $\mathfrak{G}[v](x) = \tilde{\mathfrak{G}}[v](x) + o(\gamma^2)$ given by (67) for the bulk region $x \in \mathcal{X}$. Thus, the difference $|\mathfrak{G}[v](x) - \tilde{\mathfrak{G}}[v](x)|$ converges to zero as $\gamma \rightarrow 0$ for $x \in \mathcal{X}$. ■

It is expected from Proposition 3 that the solution $\tilde{v}(x, t)$ to the partial differential equation (66) is very close to the initial state for sufficiently small γ as long as t is finite, since the initial state corresponds to the fixed-point of the integral systems (46) and (47) as $i \rightarrow \infty$. More precisely, we have the following lemma.

Lemma 5: For any $t_0 \geq 0$ and $\epsilon > 0$, there exists some $\gamma_0 > 0$ such that

$$\int_{-1}^1 |\tilde{v}(x, t_0) - \tilde{v}(x, 0)| dx < \epsilon, \quad (74)$$

for all $\gamma \in (0, \gamma_0)$.

Proof: See Appendix C for a proof based on Proposition 3. ■

We are ready to prove Theorem 5.

Proof of Theorem 5: Let $v_\gamma(x) = \lim_{i \rightarrow \infty} v_\gamma(x, i)$ and $\tilde{v}(x) = \lim_{t \rightarrow \infty} \tilde{v}(x, t)$. From Lemma 1 and the first property of Lemma 2, for any $x \in [-1, 1]$, $l \in \mathcal{L}$, and $\epsilon > 0$ there exists some $I \in \mathbb{N}$ such that

$$|v_l(i) - v_l(I)| < \epsilon, \quad (75)$$

$$|v_\gamma(x, i) - v_\gamma(x, I)| < \epsilon, \quad (76)$$

for all $i \geq I$. For this number I of iterations and $x_l = (2l/L) - 1$, we use the triangle inequality and (75) to obtain

$$\begin{aligned} &\frac{1}{L} \sum_{l \in \mathcal{L}} |v_l(i) - \tilde{v}(x_l)| \\ &< \frac{1}{L} \sum_{l \in \mathcal{L}} |v_l(I) - v_\gamma(x_l, I)| + \frac{1}{L} \sum_{l \in \mathcal{L}} |v_\gamma(x_l, I) - \tilde{v}(x_l)| + \epsilon. \end{aligned} \quad (77)$$

The last property of Lemma 2 implies that the first term on the upper bound (77) tends to zero in the continuum limit. From the definition of the Riemann integral, the sum $L^{-1} \sum_{l \in \mathcal{L}}$ in the second term can be replaced by the integral $2^{-1} \int_{-1}^1 dx$. More precisely, we have

$$\begin{aligned} \lim_{W=\gamma L \rightarrow \infty} \frac{2}{L} \sum_{l \in \mathcal{L}} |v_\gamma(x_l, I) - \tilde{v}(x_l)| \\ = \int_{-1}^1 |v_\gamma(x, I) - \tilde{v}(x)| dx. \end{aligned} \quad (78)$$

From (76) we have the following bound for the integrand

$$|v_\gamma(x, I) - \tilde{v}(x)| < |v_\gamma(x) - \tilde{v}(x)| + \epsilon. \quad (79)$$

Applying these observations to (77) yields

$$\begin{aligned} \lim_{\gamma \rightarrow 0} \lim_{I \rightarrow \infty} \lim_{W=\gamma L \rightarrow \infty} \frac{1}{L} \sum_{l \in \mathcal{L}} |v_l(i) - \tilde{v}(x_l)| \\ < \frac{1}{2} \lim_{\gamma \rightarrow 0} \int_{-1}^1 |v_\gamma(x) - \tilde{v}(x)| dx + 2\epsilon. \end{aligned} \quad (80)$$

Thus, it is sufficient to prove that the first term on the upper bound (80) is equal to zero.

Lemma 4 implies that $\tilde{v}(x, t)$ converges uniformly to $\tilde{v}(x)$ as $t \rightarrow \infty$ with respect to $\gamma > 0$. Since $|\tilde{v}(x, t) - \tilde{v}(x)|$ is bounded, from the dominated convergence theorem we find that for any $\epsilon_1 > 0$ there exists some $t_0 > 0$ such that

$$\frac{1}{2} \int_{-1}^1 |\tilde{v}(x, t) - \tilde{v}(x)| dx < \epsilon_1, \quad (81)$$

for all $t \geq t_0$ and $\gamma > 0$. From this observation, we use the triangle inequality to obtain

$$\frac{1}{2} \int_{-1}^1 |v_\gamma(x) - \tilde{v}(x)| dx < \frac{1}{2} \int_{-1}^1 |v_\gamma(x) - \tilde{v}(x, t_0)| dx + \epsilon_1. \quad (82)$$

From the initial condition $|\tilde{v}(x, 0) - v_\gamma(x)| < \epsilon_{\text{init}}$, Lemma 5 implies that the first term on the upper bound converges to zero as $\gamma \rightarrow 0$. Thus, the upper bound (80) tends to zero. ■

B. Review of Phenomenological Study

We shall review our phenomenological study on spatial coupling [29]. This section is organized as an independent section of Section V-A. The study characterizes the position of the BP threshold for SC systems. Furthermore, it helps us understand why spatial coupling improves the conventional BP threshold. We first explain the dynamics of the partial differential equation (62), although it is sufficient to investigate the properties of stationary solutions from Theorem 5.

We start with the following partial differential equation:

$$\frac{\partial u}{\partial t} = A(u(x, t)) \{-V'(u(x, t)) + \gamma^2 \mathcal{L}[u(\cdot, t)](x)\}, \quad (83)$$

with \mathcal{L} defined in (60). In (83), $t \geq 0$ and $x \in (-1, 1)$ denote the temporal and spatial variables, respectively. The state $u(x, t)$ is associated with a performance measure, such as SIR, ME, and so on. Without loss of generality, we assume that larger u implies better performance. The parameter $\gamma > 0$

represents the *strength* of spatial coupling. The dynamics of the uncoupled system $\gamma = 0$ is characterized by a potential energy function $V(u)$, which is assumed to be bounded below. The two functions $A(u) > 0$ and $B(u) > 0$ in (60) and (83) are arbitrary smooth functions. These assumptions hold for the CDMA case, in which $\psi(v) = -\zeta(v)$ and $\phi(u) = 1/(\sigma_n^2 - u)$ for $u < 0$.

Let us consider the uncoupled system $\gamma = 0$. In this case, the partial differential equation (83) reduces to the ordinary differential equation

$$\frac{\partial u}{\partial t} = -A(u)V'(u). \quad (84)$$

Since the state $u(x, t)$ does not depend on the spatial variable x anymore, we re-write it as $u(t)$ for the uncoupled system. It is straightforward to find

$$\frac{d}{dt} V(u(t)) = -A(u)\{V'(u(t))\}^2 \leq 0, \quad (85)$$

where the equality holds if and only if $V'(u(t)) = 0$. This implies that the energy $V(u(t))$ monotonically decreases with the time-evolution of the state $u(t)$. Since the potential is bounded below, the state $u(t)$ converges to a (local) minimum of the potential $V(u)$ as $t \rightarrow \infty$.

Suppose that the potential $V(u)$ has a parameter β , and that the shape of the potential as a function of u changes with the increase of β , as shown in Fig. 1. The potential $V(u)$ is assumed to have the unique stable solution for small β . As β increases across a critical value of β , denoted by β_{BP} , a metastable solution emerges to the left side of the global stable solution. The BP threshold for the uncoupled system $\gamma = 0$ is defined as the supremum of β_{th} such that the state converges to the rightmost stable solution as $t \rightarrow \infty$ for all $\beta \in (0, \beta_{\text{th}})$. When the initial state is smaller than the infimum of the unstable solution of $V(u)$ over all $\beta > \beta_{\text{BP}}$, the BP threshold is equal to the critical value β_{BP} such that the potential $V(u)$ is monostable (resp. bistable) for all $\beta < \beta_{\text{BP}}$ (resp. $\beta > \beta_{\text{BP}}$). In fact, the state for the uncoupled system $\gamma = 0$ is trapped in the left stable solution for $\beta > \beta_{\text{BP}}$, since the initial state is smaller than the unstable solution of $V(u)$, whereas it can arrive at the rightmost stable solution for $\beta < \beta_{\text{BP}}$. Spatial coupling allows the state to escape from the left stable solution and to arrive at the right stable solution for $\beta \in (\beta_{\text{BP}}, \tilde{\beta}_{\text{BP}}^{(\text{SC})})$, in which $\tilde{\beta}_{\text{BP}}^{(\text{SC})}$ is called potential threshold, whereas the state may be trapped in the left stable solution for $\beta > \tilde{\beta}_{\text{BP}}^{(\text{SC})}$. The goal of this section is to elucidate the mechanism of escaping from the left stable solution and to specify the position of the potential threshold $\tilde{\beta}_{\text{BP}}^{(\text{SC})}$. We hereafter focus on the case $\beta > \beta_{\text{BP}}$, in which the potential $V(u)$ is bistable.

Let u_l and u_r denote the left (smaller) and right (larger) stable solutions of $V(u)$, respectively. The boundaries of the state $u(x, t)$ are assumed to be fixed to the right stable solution, i.e. $u(\pm 1, t) = u_r$ for all $t \geq 0$. The *correct* boundary condition $u(\pm 1, t) = u_{\text{max}}$ will be considered shortly. Furthermore, we impose an initial condition $u(x, 0) = u_{\text{init}}(x)$, with some function $u_{\text{init}}(x)$. The state $u(x, t)$ governed by (83) moves around in a space of functions on $[-1, 1]$ as t increases.

If $u_{\text{init}}(x)$ is smaller than the unstable solution of $V(u)$ for any $x \in (-1, 1)$, the state for the uncoupled system $\gamma = 0$ is trapped in $u(x) = u_l$ for all $x \in (-1, 1)$. Why can the state escape from the left stable solution for SC systems? When can the state arrive at the right stable solution u_r for all x as $t \rightarrow \infty$? Our phenomenological study provides answers to these questions.

In order to answer the former question, we represent the system (83) as a gradient system

$$\frac{\partial u}{\partial t} = -A(u(x, t)) \frac{\delta H}{\delta u}[u(\cdot, t)](x), \quad (86)$$

where the energy functional $H[u]$ is given by

$$H[u] = \int_{-1}^1 \left[V(u(x)) + \frac{\gamma^2 B(u(x))}{2} \left(\frac{\partial u}{\partial x} \right)^2 \right] dx. \quad (87)$$

In (86), $\delta/\delta u$ denotes the functional derivative with respect to u . See Appendix B for the derivation of (86). As shown in the same appendix, it is straightforward to find

$$\frac{dH}{dt}[u(\cdot, t)] = - \int_{-1}^1 A(u(x, t)) \left(\frac{\delta H}{\delta u}[u(\cdot, t)](x) \right)^2 dx \leq 0, \quad (88)$$

where the equality holds if and only if $\delta H/\delta u = 0$. This implies that the energy functional (87) monotonically decreases with the time-evolution of the state. Since (87) is bounded below, $H[u(\cdot, t)]$ converges to a finite value as $t \rightarrow \infty$. Thus, the state $u(x, t)$ is guaranteed to converge to a stationary state $u(x)$ as $t \rightarrow \infty$, which is a local minimum of the energy functional (87). It is obvious that the uniform solution $u(x) = u_r$ is a stable stationary solution to (86), since the boundaries are fixed to the right stable solution u_r . The second term in the integrand of (87) smooths the state $u(x, t)$ spatially. This smoothing effect helps the state escape from the left stable solution and move toward the uniform solution for all $x \in [-1, 1]$. Surprisingly, the smoothing effect will be shown to work even in the limit $\gamma \rightarrow 0$.

We next elucidate the answer to the latter question. The following theorem presents a partial answer to the question.

Theorem 6: Suppose that the boundary is fixed to the right stable solution u_r of the potential $V(u)$. If and only if u_r is the unique global stable solution of $V(u)$, the uniform solution $u(x) = u_r$ is the unique stationary solution to the system (83) in the limit $\gamma \rightarrow 0$.

Proof: See Section V-C. ■

As shown from (88), the state $u(x, t)$ converges to a stable stationary solution as $t \rightarrow \infty$. Combining this observation and Theorem 6 implies that the state $u(x, t)$ converges to the uniform solution if u_r is the unique global stable solution of the potential $V(u)$. In other words, the state $u(x, t)$ can escape from the left stable solution and arrive at the right stable solution u_r for all x , when u_r is the unique global stable solution of the potential $V(u)$.

Recall that the shape of the potential $V(u)$ with a positive parameter β is assumed to change with the increase of β , as shown in Fig. 1. The BP threshold for the SC system is defined as the parameter β_{th} such that the state $u(x, t)$

converges to the uniform solution for $\beta < \beta_{\text{th}}$, whereas it is trapped in a non-uniform stationary solution for $\beta > \beta_{\text{th}}$. Suppose that $V(u_l) = V(u_r)$ holds at $\beta = \tilde{\beta}_{\text{BP}}^{(\text{SC})}$. Theorem 6 implies that $\tilde{\beta}_{\text{BP}}^{(\text{SC})}$ is a lower bound on the BP threshold, since the state is guaranteed to converge to the uniform solution for $\beta < \tilde{\beta}_{\text{BP}}^{(\text{SC})}$.

It depends on the initial condition $u(x, 0) = u_{\text{init}}(x)$ whether $\tilde{\beta}_{\text{BP}}^{(\text{SC})}$ is equal to the BP threshold. In other words, it depends on the initial condition whether the state converges to a stable non-uniform solution when the non-uniform solution exists. As a trivial example, let us consider the initial condition $u_0(x) = u_r$. Even if there is a non-uniform stationary solution to (83) the state $u(x, t)$ never converges to the non-uniform solution as $t \rightarrow \infty$, since the initial state is a stable stationary solution to (83). When the initial state is smaller than the left stable solution u_l in a bulk region far from the boundaries, on the other hand, the state is expected to converge toward a stable non-uniform stationary solution if the non-uniform solution exists. Unfortunately, we could not prove the convergence toward a stable non-uniform stationary solution under the latter initial condition. If we could prove it, we would be able to present the complete answer to the question: When can the state arrive at the right stable solution u_r for all x as $t \rightarrow \infty$?

Remark 3: The condition presented in Theorem 6, i.e. the global stability of the potential $V(u)$ at $u = u_r$ may not be necessary for strictly positive γ , whereas it is sufficient for any $\gamma > 0$: The uniform solution may be the unique stable stationary solution for strictly positive γ , when β is slightly larger than $\tilde{\beta}_{\text{BP}}^{(\text{SC})}$. Let us consider the limit $\gamma \rightarrow \infty$ to present an intuitive understanding of this statement. The first term in the integrand of (87) is negligible in the limit $\gamma \rightarrow \infty$. Thus, the energy functional (87) has the unique stable solution that satisfies $\partial u/\partial x = 0$ and $u(\pm 1) = u_r$ or equivalently $u(x) = u_r$. This observation implies that for sufficiently large γ the state converges to the uniform solution as $t \rightarrow \infty$, regardless of β . The smoothing effect with $\gamma > 0$, given by the second term in the integrand of (87), helps the state converge to the uniform solution for β slightly larger than $\tilde{\beta}_{\text{BP}}^{(\text{SC})}$.

Corollary 1: Suppose that the boundary is fixed to $\bar{u} > u_r$. If u_r is the unique global stable solution of $V(u)$, a solution $u(x)$ that satisfies $u(x) \geq u_r$ for all x is the unique stationary solution to the system (83) for any $\gamma > 0$.

Proof: See Section V-C. ■

Theorem 4 follows from Theorem 5 and Corollary 1.

C. Proof of Theorem 6

Let $g(u)$ denote a monotonically increasing function that satisfies

$$g'(u) = \sqrt{B(u)}. \quad (89)$$

Letting $\tilde{u} = g(u)$ transforms the system (83) into

$$\frac{\partial \tilde{u}}{\partial t} = A(u)B(u) \left[\gamma^2 \frac{\partial^2 \tilde{u}}{\partial x^2} - \frac{V'(u)}{\sqrt{B(u)}} \right], \quad (90)$$

with $u = g^{-1}(\tilde{u})$. The newly introduced variable \tilde{u} corresponds to the normal coordinate system in differential geometry [53].

Let us introduce an effective potential energy function $U(\tilde{u})$ that satisfies

$$U'(\tilde{u}) = \frac{V'(u)}{\sqrt{B(u)}}, \quad (91)$$

with $u = g^{-1}(\tilde{u})$. It is straightforward to confirm $U(\tilde{u}) = V(g^{-1}(\tilde{u})) + C$, with a constant C . Note that $\tilde{u}_r = g(u_r)$ is the global stable solution of the effective potential $U(\tilde{u})$ if and only if u_r is the global stable solution of the original one $V(u)$.

We first prove the sufficiency of Theorem 6, i.e. the uniform solution is the unique stable stationary solution if \tilde{u}_r is the unique global stable solution of $U(\tilde{u})$. The following result is valid for any $\gamma > 0$.

Theorem 7 (Takeuchi et al. 2012): Suppose that the boundary is fixed to the right stable solution \tilde{u}_r of the potential $U(\tilde{u})$. If \tilde{u}_r is the unique global stable solution of the effective potential $U(\tilde{u})$, the uniform solution $\tilde{u}(x) = \tilde{u}_r$ is the unique stationary solution to (90).

Proof of Theorem 7: We follow [29] to prove Theorem 7. A stationary solution $\tilde{u}(x)$ to (90) satisfies

$$\gamma^2 \frac{d^2 \tilde{u}}{dx^2} = U'(\tilde{u}), \quad (92)$$

with the boundary condition $\tilde{u}(\pm 1) = \tilde{u}_r$. Integrating (92) after multiplying both sides by $d\tilde{u}/dx$, we obtain

$$\frac{\gamma^2}{2} \left(\frac{d\tilde{u}}{dx} \right)^2 = U(\tilde{u}) + C, \quad (93)$$

with a constant C . Since \tilde{u}_r is the global stable solution of $U(\tilde{u})$, the boundary condition $\tilde{u}(\pm 1) = \tilde{u}_r$ and the positivity of the left-hand side (LHS) on (93) imply $C \geq -U(\tilde{u}_r)$. Let us prove $C = -U(\tilde{u}_r)$. From the symmetry of the boundary-value problem (92) with $\tilde{u}(\pm 1) = \tilde{u}_r$, any solution $\tilde{u}(x)$ is symmetric about the axis $x = 0$, i.e. an even function $\tilde{u}(-x) = \tilde{u}(x)$. The point $x = 0$ is the middle point of the interval $[-1, 1]$. Furthermore, any stationary solution $\tilde{u}(x)$ must be continuously differentiable since it is a solution to the second-order differential equation (92). Thus, we find $d\tilde{u}/dx|_{x=0} = 0$. Evaluating (93) at $x = 0$ yields $U(\tilde{u}(0)) = -C \leq U(\tilde{u}_r)$. Combining this result with the global stability of \tilde{u}_r , i.e. $U(\tilde{u}(0)) \geq U(\tilde{u}_r)$, we obtain $C = -U(\tilde{u}(0)) = -U(\tilde{u}_r)$. Note that the uniqueness of the global stable solution implies $\tilde{u}(0) = \tilde{u}_r$.

We shall show that the uniform solution $\tilde{u}(x) = \tilde{u}_r$ is the unique solution to (93) with $C = -U(\tilde{u}_r)$. We have decomposed the boundary-value problem on $[-1, 1]$ into two equivalent subproblems on $[-1, 0]$ and $[0, 1]$. Repeating this argument infinitely, we find that $\tilde{u}(x)$ is equal to \tilde{u}_r at $x = k/2^j$ for all $\{k \in \mathbb{Z} : |k| \leq 2^j\}$ and all $j \geq 0$. Since $\tilde{u}(x)$ is continuous, this observation implies $\tilde{u}(x) = \tilde{u}_r$ for all x . Thus, the uniform solution $\tilde{u}(x) = \tilde{u}_r$ is the unique solution to (93) or (92). ■

Remark 4: Hassani et al. [28] presented an intuitive argument based on classical mechanics, and obtained results

equivalent to Theorem 7. We shall review their intuitive argument. The differential equation (92) is regarded as the Newton equation of motion: The state $\tilde{u}(x)$ is regarded as the position of a particle with mass γ^2 at time x , moving subject to the potential energy $-U(\tilde{u})$. Note that x corresponds to the temporal variable in this interpretation, although x has been defined as the spatial variable in the original phenomenological system (83). Expression (93) corresponds to the conservation of mechanical energy.

The boundary condition $\tilde{u}(-1) = \tilde{u}_r$ implies that the particle is on the right maximum of the inverted potential $-U(\tilde{u})$ at time $x = -1$. The uniform solution corresponds to the situation under which the particle continues to stay on the right maximum. Can the other solutions exist? In other words, can the particle move from the initial position at time $x = -1$ and return to the initial position at time $x = 1$? Since \tilde{u}_r is the global maximizer of the inverted potential $-U(\tilde{u})$, the conservation of mechanical energy implies that the velocity $\tilde{u}'(x)$ at time $x = 0$ must be non-zero if the particle moves to some position $\tilde{u}(0) \neq \tilde{u}_r$. From the symmetry of $\tilde{u}(x)$ about the axis $x = 0$, however, the non-zero velocity $\tilde{u}'(x) \neq 0$ at time $x = 0$ indicates that $\tilde{u}(x)$ is non-differentiable at time $x = 0$. This is a contradiction, since $\tilde{u}(x)$ is the solution to the second-order differential equation (92). Thus, it is impossible for the particle to move from the initial position and to return to the initial position at time $x = 1$. These observations imply that the uniform solution $\tilde{u}(x) = \tilde{u}_r$ is the unique solution to (92).

Let us prove Corollary 1. The transformation of variables $\tilde{u} = g(u)$ maps $\tilde{u} > u_r$ to a point $g(\tilde{u})$ greater than \tilde{u}_r . Corollary 1 holds trivially from the physical intuition, since it is impossible for the particle to return to the initial position $g(\tilde{u}) > \tilde{u}_r$ when the particle gets over the hill $\tilde{u} = \tilde{u}_r$. The proof is formally given as follows:

Proof of Corollary 1: The statement holds if $\tilde{u}(x) > \tilde{u}_r$ for all x . Thus, we consider the case in which $\tilde{u}(x) \leq \tilde{u}_r$ for some x . Since the stationary solution is continuous, $\tilde{u}(x) = \tilde{u}_r$ holds at some points $x \in [0, 1]$. Let $x_0 \in [0, 1]$ denote the maximum of such points. Thus, we find $\tilde{u}(x) > \tilde{u}_r$ for all $x \in (x_0, 1]$. The symmetry of stationary solutions implies that $\tilde{u}(-x_0) = \tilde{u}_r$. This problem can be regarded as a boundary-value problem on $[-x_0, x_0] \subset [-1, 1]$ with the boundary condition $\tilde{u}(\pm x_0) = \tilde{u}_r$. Repeating the proof of Theorem 7, we find that $\tilde{u}(x) = \tilde{u}_r$ for all $x \in [-x_0, x_0]$. Thus, $\tilde{u}(x) \geq \tilde{u}_r$ holds for all x . ■

Theorem 7 implies that the sufficiency of Theorem 6 is correct. We next prove the necessity of Theorem 6, i.e. there is a stable non-uniform stationary solution in the limit $\gamma \rightarrow 0$, if \tilde{u}_r is the metastable solution of $U(\tilde{u})$. Let us focus on a non-uniform stationary solution $\tilde{u}(x)$ to (90) that satisfies $d\tilde{u}/dx < 0$ (resp. $d\tilde{u}/dx > 0$) for $x \in (-1, 0)$ (resp. $x \in (0, 1)$). The following theorem guarantees the existence of such a stable non-uniform stationary solution in the limit $\gamma \rightarrow 0$.

Theorem 8: Suppose that the boundary is fixed to the right stable solution \tilde{u}_r of the potential $U(\tilde{u})$, and that \tilde{u}_r is the metastable solution of the effective potential $U(\tilde{u})$. Let us define \tilde{u}_1 and \tilde{u}_{un} as $\tilde{u}_1 = g(u_1)$ and the point $\tilde{u}_{un} \in (\tilde{u}_1, \tilde{u}_r)$

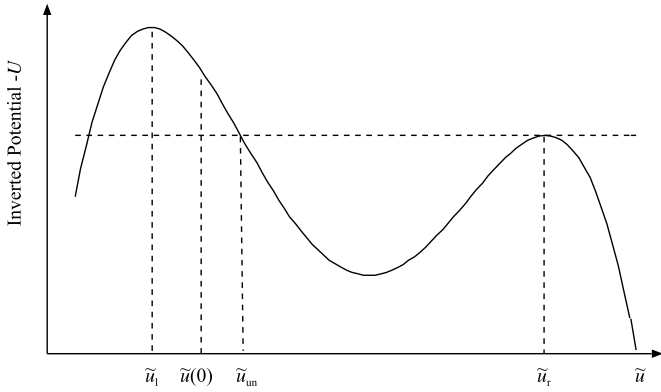


Fig. 4. Inverted potential $-U(\tilde{u})$ for $\beta > \tilde{\beta}_{\text{BP}}^{(\text{SC})}$.

satisfying $U(\tilde{u}_{\text{un}}) = U(\tilde{u}_r)$, respectively (See Fig. 4). Then, for sufficiently small $\gamma > 0$ there are two non-uniform stationary solutions $\tilde{u}_s(x)$ and $\tilde{u}_{\text{un}}(x)$ to (90). Furthermore, one stationary solution $\tilde{u}_s(x)$ converges to \tilde{u}_l for $x \in (-1, 1)$ in the limit $\gamma \rightarrow 0$. The other stationary solution $\tilde{u}_{\text{un}}(x)$ converges to \tilde{u}_r for $x \neq 0$ in the limit $\gamma \rightarrow 0$, whereas $\tilde{u}_{\text{un}}(0)$ tends to \tilde{u}_{un} in the limit $\gamma \rightarrow 0$. In particular, $\tilde{u}_s(x)$ is stable in the limit $\gamma \rightarrow 0$.

Proof of Theorem 8: See Appendix D. ■

Remark 5: The two solutions $\tilde{u}_s(x)$ and $\tilde{u}_{\text{un}}(x)$ in the limit $\gamma \rightarrow 0$ can be interpreted in terms of classical mechanics as follows: For $\tilde{u}_s(x)$, a particle starts rolling down from the right maximum of the inverted potential $-U(\tilde{u})$ toward the left maximum at time $x = -1$. The velocity is infinitely large, when the mass is infinitely small. In a moment, the particle approaches the left maximum of the inverted potential with vanishing velocity. If the approaching velocity were finite, the particle would pass through the left maximum and roll down the left cliff. At time $x = 0$, the particle starts rolling down from the left maximum toward the right maximum with infinitely small velocity. Just before time $x = 1$ the velocity becomes infinitely large, and returns to the right maximum of the inverted potential at time $x = 1$.

For the other solution $\tilde{u}_{\text{un}}(x)$, a particle starts rolling down from the right maximum of the inverted potential to the left side with infinitely small velocity at time $x = -1$. Just before time $x = 0$, the velocity of the particle becomes infinitely large, and stops at the point \tilde{u}_{un} at time $x = 0$, because of the conservation of mechanical energy. If the initial velocity were finite, the particle could not stop at the point \tilde{u}_{un} . The particle starts rolling down from the point \tilde{u}_{un} with infinitely large velocity, and approaches the right maximum with vanishing velocity at a moment. Then, the particle climbs the hill slowly, and returns to the right maximum of the inverted potential at time $x = 1$.

Theorem 8 is useful for plotting the stationary solutions to (83). Intuitively, the non-uniform solution $\tilde{u}_s(x)$ that converges to \tilde{u}_l for all $x \in (-1, 1)$ in the limit $\gamma \rightarrow 0$ represents the situation under which the state $\tilde{u}(x, t)$ is trapped around the left stable solution \tilde{u}_l as $t \rightarrow \infty$. We conjecture that $\tilde{u}_{\text{un}}(x)$ is unstable, although we could not prove the instability.

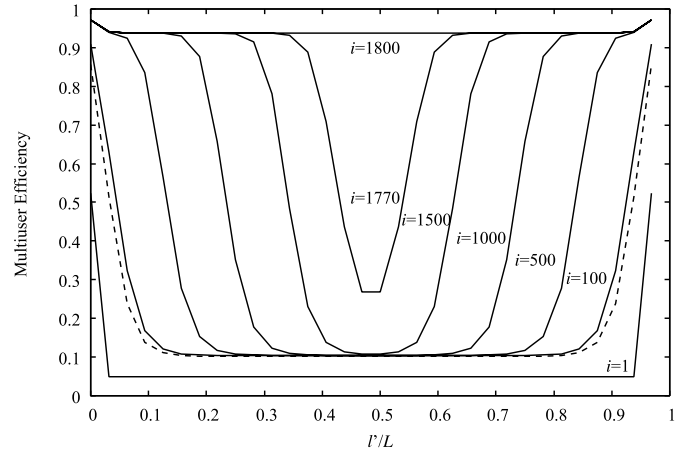


Fig. 5. Multiuser efficiency versus l'/L for $1/\sigma_n^2 = 10$ dB, $L = 32$, $W = 1$, and $\beta_{\text{init}} = 0$. The solid lines denote the MEs for $\beta = 1.97$. The dashed line shows the ME for $\beta = 1.99$ and $i = 10^5$.

VI. NUMERICAL RESULTS

A. Density-Evolution Analysis

The DE equations (26) and (27) are numerically solved to estimate the position of the BP threshold for the SC-SCDMA system. We focus on the ME $\eta_{l'}^{(i)} = \sigma_n^2 \text{sir}_{l'}^{(i)}$ in iteration i . Since the SIR $\text{sir}_{l'}^{(i)}$ must be smaller than the SNR $1/\sigma_n^2$, the ME takes a value between 0 and 1. Figure 5 shows the ME $\eta_{l'}^{(i)}$ for $\beta = 1.97$ and $\beta = 1.99$. The BP threshold $\beta_{\text{BP}}^{(\text{SC})}$ for the SC-SCDMA system based on Theorem 4 and Remark 2 is given by $\beta_{\text{BP}}^{(\text{SC})} \approx 1.98267$ for $1/\sigma_n^2 = 10$ dB. For $\beta = 1.97 < \beta_{\text{BP}}^{(\text{SC})}$, the BP receiver first obtains reliable information about the data symbols at the boundaries $l'/L = 0$ and $l'/L = 1 - 1/L$, transmitted in the initialization phase. Then, the reliable information propagates toward the middle position $l'/L = 1/2$ as i increases. Eventually, the ME tends toward an almost uniform solution, which is close to 1 for all positions l' . This result implies that the BP receiver can eliminate the MAI for $\beta = 1.97$. For $\beta = 1.99 > \beta_{\text{BP}}^{(\text{SC})}$, on the other hand, the ME tends to a non-uniform solution after many iterations: The ME for $i = 10^5$ is close to 0 around the center $l'/L = 1/2$, whereas it is close to 1 near the boundaries $l'/L = 0$ and $l'/L = 1 - 1/L$. This observation implies that the system is interference-limited for $\beta = 1.99$.

In order to investigate the convergence speed of the continuum limit, we focus on the fixed-points to the DE equations (26) and (27). See [24] for how to find the fixed-points to the DE equations (26) and (27). Figure 6 shows the ME at the center $l'/L = 1/2$, given via the fixed-points to (26) and (27). The MEs for $W = 1$ and $W = 2$ are represented by the solid and dashed lines, respectively. The dotted line shows the ME in the limit $L, W \rightarrow \infty$ with $\gamma = W/L \rightarrow 0$, based on Theorem 8. The asymptotic⁵ ME is indistinguishable from that for $W = 2$. In the limit $L, W \rightarrow \infty$ with $\gamma = W/L \rightarrow 0$ the DE equations (26) and (27) have the unique fixed-point when β is smaller than $\beta_{\text{BP}}^{(\text{SC})}$, which is shown by the vertical line, whereas there are multiple fixed-

⁵Note that the term “asymptotic” in Section VI-A implies the limit $\gamma \rightarrow 0$ after taking the continuum limit, whereas we have so far used the term to mean the large-sparse-system limit.

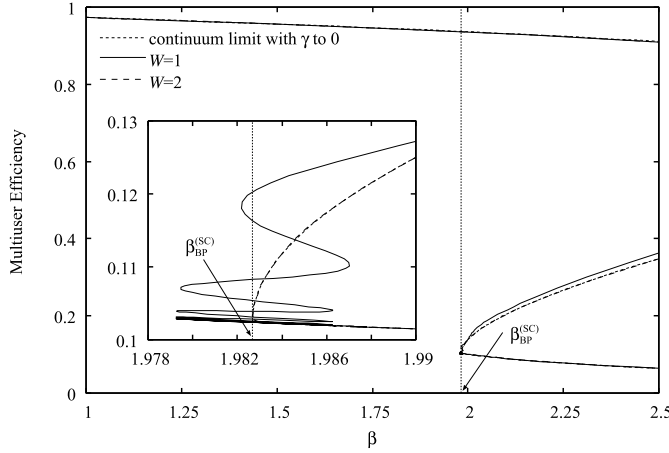


Fig. 6. Multiuser efficiency at $l'/L = 1/2$ versus β for $1/\sigma_n^2 = 10$ dB, $L = 32$, and $\beta_{\text{init}} = 0$.

TABLE I

BP THRESHOLDS FOR THE SC-SCDMA SYSTEMS. $1/\sigma_n^2 = 10$ dB AND $\beta_{\text{init}} = 1$. β_{BP} AND $\beta_{\text{BP}}^{(\text{SC})}$ ARE APPROXIMATELY GIVEN BY $\beta_{\text{BP}} \approx 1.73078$ AND $\beta_{\text{BP}}^{(\text{SC})} \approx 1.98267$, RESPECTIVELY

		W			
		1	2	3	4
L	16	1.97947	1.99150	2.04385	2.16470
	32	1.97925	1.98266	1.98321	1.98665
	64	1.97925	1.98264	1.98267	1.98267
	128	1.97925	1.98264	1.98267	1.98267

points for $\beta > \beta_{\text{BP}}^{(\text{SC})}$. The ME for $W = 1$ displays oscillating behavior around the BP threshold $\beta_{\text{BP}}^{(\text{SC})}$, as shown in the inset of Fig. 6. The same phenomenon was observed in SC-LDPC codes [24]. The wiggle decreases slightly the maximum of β at which the DE equations (26) and (27) for $W = 1$ have a unique fixed-point. Since the amplitude of the wiggle decreases rapidly with the increase of W , the ME for $W = 2$ is indistinguishable from the asymptotic one shown by the dotted line, except for a neighborhood of $\beta = \beta_{\text{BP}}^{(\text{SC})}$. This oscillating behavior around $\beta_{\text{BP}}^{(\text{SC})}$ seems to disappear in the limit $L, W \rightarrow \infty$ with $\gamma = W/L \rightarrow 0$. These observations imply that the convergence to the asymptotic ME is so fast that the asymptotic result can provide good approximations for the SC-SCDMA systems with finite L and W .

Tables I and II list the BP thresholds for the SC-SCDMA system for SNRs $1/\sigma_n^2 = 10$ dB and $1/\sigma_n^2 = 12$ dB, respectively. The thresholds were estimated by solving the DE equations (26) and (27) numerically. Note that the listed values are not the average system load $\bar{\beta}$ but the system load β in the communication phase. We find that the thresholds for $L = 16$ are larger than the BP threshold $\beta_{\text{BP}}^{(\text{SC})} \approx 1.98267$ in the limit $L, W \rightarrow \infty$ with $\gamma = W/L \rightarrow 0$, except for $W = 1$. This observation is due to strictly positive γ : When β is slightly larger than $\beta_{\text{BP}}^{(\text{SC})}$, as noted in Remark 3, the partial differential equation (83) for $\gamma > 0$ may converge to an almost uniform solution, like the solution for $i = 1800$ in Fig. 5.

We have so far investigated the static properties of the DE equations (26) and (27). We next consider the dynamic properties of the DE equations. Figure 7 shows the ME $\eta_{l'}^{(i)}$ at $l'/L = 1/2$ as a function of the number of iterations i .

TABLE II

BP THRESHOLDS FOR THE SC-SCDMA SYSTEMS. $1/\sigma_n^2 = 12$ dB AND $\beta_{\text{init}} = 1$. β_{BP} AND $\beta_{\text{BP}}^{(\text{SC})}$ ARE APPROXIMATELY GIVEN BY $\beta_{\text{BP}} \approx 1.87344$ AND $\beta_{\text{BP}}^{(\text{SC})} \approx 2.50716$, RESPECTIVELY

		W			
		1	2	3	4
L	16	2.38479	2.49386	2.53057	2.65917
	32	2.38479	2.49314	2.50589	2.50726
	64	2.38479	2.49314	2.50588	2.50705
	128	2.38479	2.49314	2.50588	2.50705

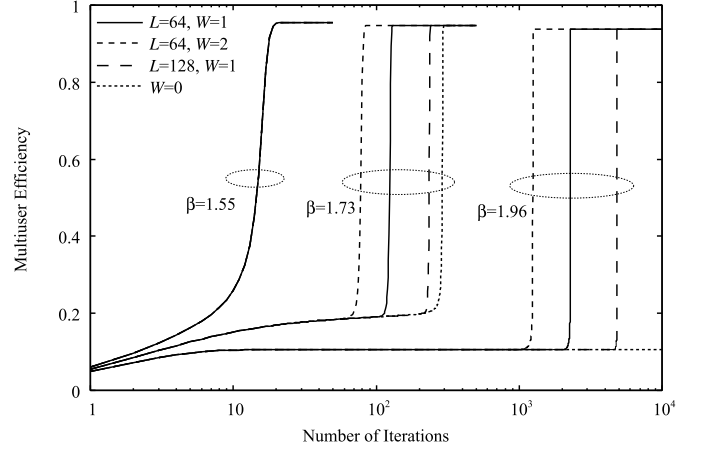


Fig. 7. Multiuser efficiency at $l'/L = 1/2$ versus the number of iterations for $1/\sigma_n^2 = 10$ dB and $\beta_{\text{init}} = 0$.

The conventional BP threshold β_{BP} is approximately equal to $\beta_{\text{BP}} \approx 1.73078$ for SNR $1/\sigma_n^2 = 10$ dB, while the BP threshold for the SC-SCDMA system is given by $\beta_{\text{BP}}^{(\text{SC})} \approx 1.98267$. The number of iterations required for convergence increases as β grows. Interestingly, the SC-SCDMA systems converge to the stationary solutions more quickly than the uncoupled system $W = 0$ for $\beta = 1.73$, whereas all systems converge at the same speed for $\beta = 1.55 < \beta_{\text{BP}}$. This observation is because the uncoupled system requires infinitely many iterations for convergence when β tends to the BP threshold β_{BP} from below. The number of iterations required for $L = 64$ and $W = 2$ is roughly half the number of iterations for $L = 64$ and $W = 1$, while the one required for $L = 128$ and $W = 1$ is roughly twice. These results are consistent with the intuition that reliable information at the boundaries $l' = 0$ and $l' = L - 1$ should propagate toward the middle position $l' = L/2$ at a speed proportional to $\gamma = W/L$.

B. Numerical Simulations

Numerical simulations of the BP receivers are presented. We first focus on uncoupled SCDMA systems, i.e. $W = 0$. Figure 8 plots the BERs of the (exact) BP receiver. The results for $r = 4, 6, 8$ are denoted by $\{+\}$, $\{\times\}$, and $\{\square\}$ connected with solid or dashed lines, respectively. The analytical results in the large-sparse-system limit are also shown by the dotted lines. When $\beta = 1$, the large-sparse-system result can provide a good approximation of the BER for $r = 4$. When $\beta = 1.45$, however, there are gaps between the large-sparse-system result and the BERs for $r = 4, 6, 8$ especially in the moderate-SNR regime. The large-sparse-system result provides a larger

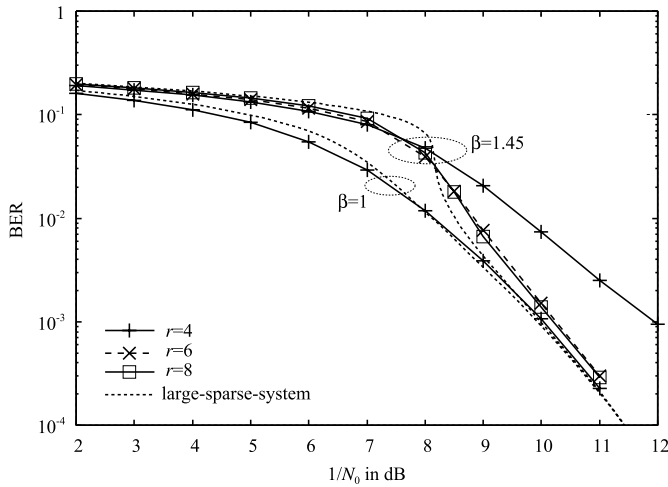


Fig. 8. BER versus SNR for $K = 1000$ and $W = 0$. The number of iterations is equal to 40.

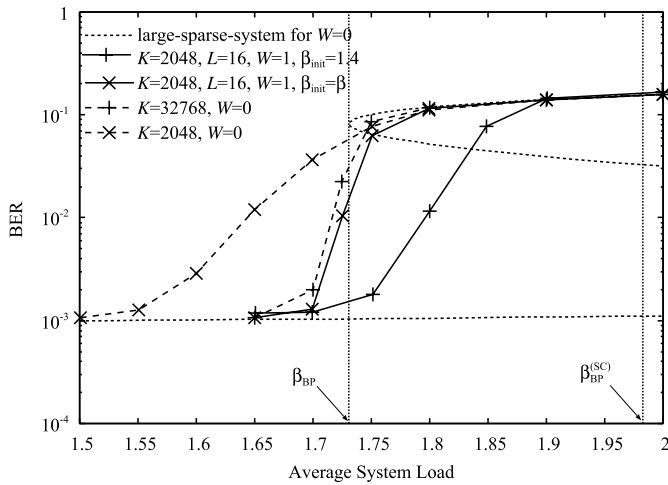


Fig. 9. BER versus average system load for $1/\sigma_n^2 = 10$ dB and $r = 32$. The number of iterations is equal to 1000.

estimate than the actual BER in the low-SNR regime, whereas it predicts a smaller BER in the high-SNR regime. These observations imply that, as the system load grows, larger r is required in order for the large-sparse-system result to provide good approximations for the actual BERs.

Figure 9 shows a comparison between the SCDMA systems with and without spatial coupling. We used the BP receiver with GA to reduce the computational complexity. The horizontal axis is the average system load given by (8). The BER at the middle position $l'/L = 1/2$ is plotted for the SC-SCDMA system. The BERs for the uncoupled SCDMA systems are denoted by $\{+\}$ or $\{ \times \}$ connected with dashed lines. The BERs for the SC-SCDMA systems are represented by $\{+\}$ or $\{ \times \}$ connected with solid lines. We find that the performance of the SC-SCDMA system with $K = 2048$, $L = 16$, $W = 1$, and $\beta_{\text{init}} = \beta$ is superior (resp. comparable) to that of the uncoupled SCDMA system with 2048 (resp. 32768) users. Note that the SC-SCDMA system performs the BP detection for every L symbol periods, whereas the uncoupled SCDMA

system does for every symbol period. However, this delay of detection does not necessarily result in the overall delay for coded systems. Since L is commonly smaller than the code length, the overall delay is dominated by the decoding delay. Thus, the comparisons between the uncoupled SCDMA system with 2048 users and the SC-SCDMA systems make sense for practical coded systems, although the detection delay for the SC-SCDMA systems is larger than for the uncoupled SCDMA system. These observations imply that the SCDMA system with one-dimensional coupling can accelerate the convergence speed toward the large-system limit, compared to the uncoupled SCDMA system with the same number of users. Furthermore, the SC-SCDMA system with $K = 2048$, $L = 16$, $W = 1$, and $\beta_{\text{init}} = 1.4$ can provide a significant improvement in BER for high system loads, compared to the SC-SCDMA system with $\beta_{\text{init}} = \beta$. The BERs for the SC-SCDMA system with $\beta_{\text{init}} = 1.4$ seem to be trapped in the top (bad) solution obtained from the large-sparse-system analysis, when the average system load is equal to 1.9. This is due to finite L , W , K , and N : Substituting the BP threshold $\beta_{\text{BP}}^{(\text{SC})} \approx 1.98267$ into β in the average system load (8), we find that the corresponding average system load is approximately equal to 1.93. The remaining gap 0.03 seems to be due to finite K and N .

In order to achieve the improved BP threshold, L must tend to infinity. Let us discuss the effect of increasing L for finite K and N . If K and N were infinity, reliable information at the boundaries $l' = 0$ and $l' = L - 1$ could propagate to the adjacent positions successfully. For finite K and N , however, it is probabilistic whether reliable information can propagate to the adjacent positions successfully. As L increases, thus, it becomes difficult for reliable information to propagate to the middle position successfully. Increasing K and N results in a reduction of the probability with which the propagation of reliable information to the adjacent positions fails. These arguments imply that the system size required for achieving a BER close to the analytical one increases as the average system load gets closer to the improved BP threshold.

VII. CONCLUSIONS

The SC-SCDMA system has been proposed to improve the performance of iterative MUD based on BP. We have derived the two iterative receivers, one based on exact BP, and the other on approximate BP with GA. The two BP receivers can achieve the same performance in the large-sparse-system limit. The analysis of the DE equations for the two receivers implies that the BP threshold can be improved up to the IO threshold by spatial coupling. Numerical simulations imply that spatial coupling can provide a significant improvement in BER for a fixed finite-sized system especially in the region of high system loads, whereas a quite large system is required for approaching the IO threshold.

We remark a capability of the phenomenological methodology for specifying the BP threshold for SC systems and a direction of future work to conclude this paper. The phenomenological result presented in Section V is applicable to characterizing the BP threshold for any SC system, if

DE equations for the corresponding uncoupled system are described by one parameter and if DE equations for the SC system is included in the DE equations (41) and (42). Of course, the presented method is not applicable to all SC systems. A further generalization of the phenomenological model is left as a future work.

APPENDIX A PROOF OF THEOREM 1

A. Reparametrization

In order to prove Theorem 1, we evaluate the evolution of the tentative marginal posterior probability (12) in the large-sparse-system limit, following [23], [54]. The marginal posterior probability is a random variable on the space of probability distributions, because of the randomness of \mathcal{Y} and \mathbf{G} . Since we have assumed BPSK, the marginal posterior probability (12) can be represented with one parameter. Selecting the log likelihood ratio (LLR) as the parameter is suitable for proving Theorem 1. Evaluating the evolution of the tentative marginal posterior probability (12) is equivalent to tracing the evolution of the pdf of the LLR.

Let $L_{(n,l) \rightarrow (k,l')}^{(i)}$ denote the LLR for the message (13) provided from the function node (n, l) to the variable node (k, l') in iteration i ,

$$L_{(n,l) \rightarrow (k,l')}^{(i)} = \ln \frac{q_{n,l}^{(i)}(b_{k,l'} = 1)}{q_{n,l}^{(i)}(b_{k,l'} = -1)}. \quad (94)$$

Furthermore, we write the LLR for the message (14) propagating along the same edge in the opposite direction as

$$L_{(k,l') \rightarrow (n,l)}^{(i)} = \ln \frac{m_{n,l}^{(i)}(b_{k,l'} = 1)}{m_{n,l}^{(i)}(b_{k,l'} = -1)}. \quad (95)$$

The product step (14) can be represented as follows:

$$L_{(k,l') \rightarrow (n,l)}^{(i)} = \sum_{(\tilde{n}, \tilde{l}) \in \partial(k,l') \setminus (n,l)} L_{(\tilde{n}, \tilde{l}) \rightarrow (k,l')}^{(i)}. \quad (96)$$

The ACF property of the (r, L, W) -ensemble presented in Example 3 guarantees that the incoming LLRs $\{L_{(\tilde{n}, \tilde{l}) \rightarrow (k,l')}^{(i)}\}$ are independent random variables in the large-system limit. Furthermore, the central limit theorem implies that the LLR (96) converges in law to a Gaussian random variable in the large-sparse-system limit, i.e. in the dense limit after taking the large-system limit. Thus, it is sufficient to evaluate the mean and variance of the LLR (96) conditioned on the data symbols $\{b_{k,l'}\}$ in the large-sparse-system limit. In the proof of Theorem 1, we always fix the data symbols and omit conditioning with respect to the data symbols.

B. Density Evolution

1) *Mean and Variance of (96)*: In order to calculate the mean and variance of the LLR (96), we first define and calculate several quantities. Let us define $f_j(y)$ and $\tilde{f}_j^{(i)}(y)$

as

$$f_j(y) = \left(\frac{y - I_{n,l,k,l'}}{\sigma_n^2} \right)^j g(y - I_{n,l,k,l'}; \sigma_n^2) \quad \text{for } j = 0, 1, \quad (97)$$

$$\begin{aligned} \tilde{f}_j^{(i)}(y) = & \sum_{\{\tilde{b}_{\tilde{k}, \tilde{l}'}^{(i)}\}} \left\{ \left(\frac{y - \tilde{I}_{n,l,k,l'}^{(i)}}{\sigma_n^2} \right)^j - \frac{\delta_{j,2}}{\sigma_n^2} \right\} \\ & \cdot g(y - \tilde{I}_{n,l,k,l'}^{(i)}; \sigma_n^2) \prod_{(\tilde{k}, \tilde{l}') \in \partial(n,l) \setminus (k,l')} m_{n,l}^{(i)}(\tilde{b}_{\tilde{k}, \tilde{l}'}^{(i)}), \end{aligned} \quad (98)$$

for $j = 0, 1, 2$. In (97) and (98), $\tilde{I}_{n,l,k,l'}^{(i)}$ and $I_{n,l,k,l'}$ are given by (15) and

$$I_{n,l,k,l'} = \sum_{(\tilde{k}, \tilde{l}') \in \partial(n,l) \setminus (k,l')} \frac{s_{n,l,\tilde{k},\tilde{l}'} b_{\tilde{k}, \tilde{l}'}}{\sqrt{(W+1)\tilde{c}_{l,\tilde{k},\tilde{l}'}}}, \quad (99)$$

respectively. Furthermore, $g(x; \sigma^2)$ denotes the pdf (1) for a zero-mean Gaussian random variable with variance σ^2 . The two quantities (97) and (98) are used to Taylor-expand the RHS of (13) in the large-system limit.

Lemma 6: Suppose that (7) is picked up from the (r, L, W) -ensemble, presented in Example 3. Then,

$$\overline{\int_{-\infty}^{\infty} \frac{\tilde{f}_1^{(i-1)}(y)}{\tilde{f}_0^{(i-1)}(y)} f_1(y) dy} \rightarrow \frac{1}{\tilde{\sigma}_l^2(i)}, \quad (100)$$

$$\overline{\int_{-\infty}^{\infty} \left(\frac{\tilde{f}_1^{(i-1)}(y)}{\tilde{f}_0^{(i-1)}(y)} \right)^2 f_0(y) dy} \rightarrow \frac{\sigma_l^2(i)}{\tilde{\sigma}_l^4(i)}, \quad (101)$$

in the large-sparse-system limit, where the overlines in (100) and (101) represent the expectation with respect to (7). In the RHSs of (100) and (101), $\sigma_l^2(i)$ and $\tilde{\sigma}_l^2(i)$ are respectively given by

$$\sigma_l^2(i) = \sigma_n^2 + \frac{\beta_l}{W+1} \sum_{l'=0}^W \xi_{(l-l')_L}^{(i-1)}, \quad (102)$$

$$\tilde{\sigma}_l^2(i) = \sigma_n^2 + \frac{\beta_l}{W+1} \sum_{l'=0}^W \tilde{\xi}_{(l-l')_L}^{(i-1)}, \quad (103)$$

with

$$\xi_{l'}^{(i)} = \mathbb{E} \left[\left(b_{1,l'} - \mathbb{E}[\tilde{b}_{1,l'}^{(i)}] \right)^2 \right], \quad (104)$$

$$\tilde{\xi}_{l'}^{(i)} = \mathbb{E} \left[\left(\tilde{b}_{1,l'}^{(i)} - \mathbb{E}[\tilde{b}_{1,l'}^{(i)}] \right)^2 \right]. \quad (105)$$

In (102) and (103), $\beta_l = K/N_l$ is equal to β_{init} for $l = 0, \dots, W-1$ and to β for $l = W, \dots, L-1$, respectively.

Proof of Lemma 6: As we have noted in Section III-B, the central limit theorem implies that the postulated interference (15) converges in law to a Gaussian random variable in the dense limit. The mean and variance of (15) are given by (16) and (17), respectively. Since (98) depends on $\{\tilde{b}_{\tilde{k}, \tilde{l}'}^{(i)}\}$ only through the postulated interference (15), we calculate the

marginalization in (98) as the expectation with respect to the postulated interference to obtain

$$\tilde{f}_0^{(i-1)}(y) = g(y - \tilde{\mu}_{n,l,k,l'}^{(i-1)}; \sigma_n^2 + \tilde{v}_{n,l,k,l'}^{(i-1)}), \quad (106)$$

$$\tilde{f}_1^{(i-1)}(y) = \frac{y - \tilde{\mu}_{n,l,k,l'}^{(i-1)}}{\sigma_n^2 + \tilde{v}_{n,l,k,l'}^{(i-1)}} g(y - \tilde{\mu}_{n,l,k,l'}^{(i-1)}; \sigma_n^2 + \tilde{v}_{n,l,k,l'}^{(i-1)}), \quad (107)$$

where $\tilde{\mu}_{n,l,k,l'}^{(i)}$ and $\tilde{v}_{n,l,k,l'}^{(i)}$ are given by (16) and (17), respectively. Substituting these expressions into (100) and (101) and performing the integrations with respect to y , we have

$$\int_{-\infty}^{\infty} \frac{\tilde{f}_1^{(i-1)}(y)}{\tilde{f}_0^{(i-1)}(y)} f_1(y) dy \rightarrow \frac{1}{\sigma_n^2 + \tilde{v}_{n,l,k,l'}^{(i-1)}}, \quad (108)$$

$$\int_{-\infty}^{\infty} \left(\frac{\tilde{f}_1^{(i-1)}(y)}{\tilde{f}_0^{(i-1)}(y)} \right)^2 f_0(y) dy \rightarrow \frac{\sigma_n^2 + (I_{n,l,k,l'} - \tilde{\mu}_{n,l,k,l'}^{(i-1)})^2}{(\sigma_n^2 + \tilde{v}_{n,l,k,l'}^{(i-1)})^2}, \quad (109)$$

in the large-sparse-system limit.

In order to complete the proof, we take the expectation with respect to (7), picked up from the (r, L, W) -ensemble. The weak law of large numbers implies that the variance (17) converges in probability to the second term on the RHS of (103) in the large-sparse-system limit. Since the RHS of (108) is bounded, this implies that (100) holds. Next, the average of $(I_{n,l,k,l'} - \tilde{\mu}_{n,l,k,l'}^{(i-1)})^2$ over (7) is equal to

$$\overline{(I_{n,l,k,l'} - \tilde{\mu}_{n,l,k,l'}^{(i-1)})^2} = \sum_{(\tilde{k}, \tilde{l}') \in \partial(n, l) \setminus (k, l')} \frac{(b_{\tilde{k}, \tilde{l}'} - \mathbb{E}[\tilde{b}_{\tilde{k}, \tilde{l}'}^{(i-1)}])^2}{(W+1)\tilde{c}_{l,k,l'}}, \quad (110)$$

which converges in probability to the second term on the RHS of (102) in the large-sparse-system limit. This observation implies that (101) holds. ■

We shall evaluate the mean and variance of the LLR (96) in the large-sparse-system limit. For that purpose, we use Lemma 6 to calculate (94) up to $O(r^{-1})$. Expanding the RHS of (13) with respect to $s_{n,l,k,l'} b_{k,l'} / \sqrt{(W+1)\tilde{c}_{l,k,l'}}$ up to the second order yields

$$\begin{aligned} q_{n,l}^{(i)}(b_{k,l'}) &= \tilde{f}_0^{(i-1)}(y_{n,l}) + \tilde{f}_1^{(i-1)}(y_{n,l}) \frac{s_{n,l,k,l'} b_{k,l'}}{\sqrt{(W+1)\tilde{c}_{l,k,l'}}} \\ &\quad + \frac{\tilde{f}_2^{(i-1)}(y_{n,l})}{2} \frac{s_{n,l,k,l'}^2 b_{k,l'}^2}{(W+1)\tilde{c}_{l,k,l'}} + O(r^{-3/2}), \end{aligned} \quad (111)$$

where $\tilde{f}_j^{(i)}(y)$ is given by (98). Note that $\{b_{\tilde{k}, \tilde{l}'} : (\tilde{k}, \tilde{l}') \in \partial(n, l) \setminus (k, l')\}$ in (13) are dummy variables, so that we have replaced them by $\{\tilde{b}_{\tilde{k}, \tilde{l}'}^{(i)}\}$ to obtain (111). Substituting (111) into (94) and expanding the obtained formula, we have

$$L_{(n,l) \rightarrow (k,l')}^{(i)} = \frac{\tilde{f}_1^{(i-1)}(y_{n,l})}{\tilde{f}_0^{(i-1)}(y_{n,l})} \frac{2s_{n,l,k,l'}}{\sqrt{(W+1)\tilde{c}_{l,k,l'}}} + O(r^{-3/2}). \quad (112)$$

We note that no term proportional to r^{-1} appears under the BPSK assumption, whereas the term does for general data symbols [23], [54].

In order to calculate the mean and variance of (112), we use the following expansion:

$$\begin{aligned} p\left(y_{n,l} \left| \frac{s_{n,l,k,l'} b_{k,l'}}{\sqrt{(W+1)\tilde{c}_{l,k,l'}}} + I_{n,l,k,l'} \right.\right) \\ = f_0(y_{n,l}) + f_1(y_{n,l}) \frac{s_{n,l,k,l'} b_{k,l'}}{\sqrt{(W+1)\tilde{c}_{l,k,l'}}} + O(r^{-1}). \end{aligned} \quad (113)$$

Evaluating the mean of (112) with this expression, we obtain

$$\begin{aligned} \mathbb{E}[L_{(n,l) \rightarrow (k,l')}^{(i)}] &= \int_{-\infty}^{\infty} \frac{\tilde{f}_1^{(i-1)}(y_{n,l})}{\tilde{f}_0^{(i-1)}(y_{n,l})} f_1(y_{n,l}) dy_{n,l} \frac{2b_{k,l'}}{(W+1)\tilde{c}_{l,k,l'}} + O(r^{-3/2}) \\ &= \frac{2}{(W+1)\tilde{c}_{l,k,l'} \tilde{\sigma}_l^2(i)} b_{k,l'} + O(r^{-3/2}), \end{aligned} \quad (114)$$

where we have used (100) in the derivation of the last equality. Similarly, we use (101) to calculate the variance of (112) as

$$\mathbb{V}[L_{(n,l) \rightarrow (k,l')}^{(i)}] = \frac{4\sigma_l^2(i)}{(W+1)\tilde{c}_{l,k,l'} \tilde{\sigma}_l^4(i)} + O(r^{-3/2}). \quad (115)$$

The two expressions (114) and (115) imply that the mean and variance of the LLR (96) converge to

$$\mathbb{E}[L_{(k,l') \rightarrow (n,l)}^{(i)}] \rightarrow 2\tilde{\text{sir}}_{l'}^{(i)} b_{k,l'}, \quad (116)$$

$$\mathbb{V}[L_{(k,l') \rightarrow (n,l)}^{(i)}] \rightarrow 4\text{sir}_{l'}^{(i)}, \quad (117)$$

in the large-sparse-system limit, respectively, with

$$\text{sir}_{l'}^{(i)} = \frac{1}{W+1} \sum_{\tilde{l}=0}^W \frac{\sigma_{(\tilde{l}+l')_L}^2(i)}{\tilde{\sigma}_{(\tilde{l}+l')_L}^4(i)}, \quad (118)$$

$$\tilde{\text{sir}}_{l'}^{(i)} = \frac{1}{W+1} \sum_{\tilde{l}=0}^W \frac{1}{\tilde{\sigma}_{(\tilde{l}+l')_L}^2(i)}, \quad (119)$$

where $\sigma_l^2(i)$ and $\tilde{\sigma}_l^2(i)$ are given by (102) and (103), respectively. In the derivation of (118) and (119), we have used the assumption that (7) is picked up from the (r, L, W) -ensemble presented in Example 3.

In summary, the LLR (96) converges in law to a Gaussian random variable with mean (116) and variance (117) in the large-sparse-system limit.

2) *Decoupling*: We shall present the asymptotic expression of the equivalent channel $p(b_{k,l'}^{(i)} | b_{k,l'})$ given by (19). Let $z_{k,l'}^{(i)}$ denote a Gaussian random variable with mean $b_{k,l'}$ and variance $\text{sir}_{l'}^{(i)} / (\tilde{\text{sir}}_{l'}^{(i)})^2$. The LLR of the tentative marginal posterior probability (12) is statistically equivalent to the LLR (96) or $2\tilde{\text{sir}}_{l'}^{(i)} z_{k,l'}^{(i)}$ in the large-sparse-system limit. Since the pmf $p(x)$ for the BPSK random variable $x \in \{1, -1\}$

is proportional to $\exp(Lx/2)$, with $L = \ln\{p(x = 1)/p(x = -1)\}$, we obtain

$$\begin{aligned} p(b_{k,l'}^{(i)}|b_{k,l'}) &\propto \mathbb{E}_{z_{k,l'}^{(i)}} \left[\exp \left(\tilde{\text{sir}}_{l'}^{(i)} z_{k,l'}^{(i)} b_{k,l'}^{(i)} \right) \right] \\ &\propto \int p(b_{k,l'}^{(i)}|z_{k,l'}^{(i)}) g \left(z_{k,l'}^{(i)} - b_{k,l'}^{(i)}; \frac{\text{sir}_{l'}^{(i)}}{(\tilde{\text{sir}}_{l'}^{(i)})^2} \right) dz_{k,l'}^{(i)}, \end{aligned} \quad (120)$$

in the large-sparse-system limit, where the posterior probability $p(b_{k,l'}^{(i)}|z_{k,l'}^{(i)})$ is given by

$$p(b_{k,l'}^{(i)}|z_{k,l'}^{(i)}) = \frac{g(z_{k,l'}^{(i)} - b_{k,l'}^{(i)}; (\tilde{\text{sir}}_{l'}^{(i)})^{-1})}{p(z_{k,l'}^{(i)}; (\tilde{\text{sir}}_{l'}^{(i)})^{-1})}, \quad (121)$$

with

$$p(z_{k,l'}^{(i)}; (\tilde{\text{sir}}_{l'}^{(i)})^{-1}) = \sum_{b_{k,l'}^{(i)} = \pm 1} g(z_{k,l'}^{(i)} - b_{k,l'}^{(i)}; (\tilde{\text{sir}}_{l'}^{(i)})^{-1}). \quad (122)$$

In order to prove that the equivalent channel (120) is equal to (25), we show that $\text{sir}_{l'}^{(i)}$ is given by (26) and that $\tilde{\text{sir}}_{l'}^{(i)}$ is equal to $\text{sir}_{l'}^{(i)}$. Since the LLR (96) is statistically equivalent to $2\tilde{\text{sir}}_{l'}^{(i)} z_{k,l'}^{(i)}$ in the large-sparse-system limit, the MSE (104) and the posterior variance (105) are equal to

$$\xi_{l'}^{(i)} = \mathbb{E} \left[\left(b_{1,l'} - \langle b_{1,l'} \rangle \right)^2 \right], \quad (123)$$

$$\tilde{\xi}_{l'}^{(i)} = \mathbb{E} \left[\left(b_{1,l'}^{(i)} - \langle b_{1,l'}^{(i)} \rangle \right)^2 \right], \quad (124)$$

where the posterior mean $\langle b_{k,l'}^{(i)} \rangle$ is given by

$$\langle b_{k,l'}^{(i)} \rangle = \sum_{b_{k,l'}^{(i)} = \pm 1} b_{k,l'}^{(i)} p(b_{k,l'}^{(i)}|z_{k,l'}^{(i)}). \quad (125)$$

Expressions (102), (103), (118), (119), (123), and (124) provide DE equations with respect to $\text{sir}_{l'}^{(i)}$ and $\tilde{\text{sir}}_{l'}^{(i)}$. The initial condition $m_{n,l}^{(0)}(b_{k,l'}) = 1/2$ implies $\xi_{l'}^{(0)} = \tilde{\xi}_{l'}^{(0)} = 1$, because of $\mathbb{E}[\tilde{b}_{k,l'}^{(0)}] = 0$.

Let us prove that the DE equations reduce to those presented in Theorem 1 by induction. When $i = 1$, (102) and (103) implies $\sigma_l^2(1) = \tilde{\sigma}_l^2(1)$, given by (27) with $i = 1$. Furthermore, $\text{sir}_{l'}^{(1)} = \tilde{\text{sir}}_{l'}^{(1)}$, given by (26), holds from (118) and (119). Next, suppose that the statement holds for iteration i . Since $\text{sir}_{l'}^{(i)} = \tilde{\text{sir}}_{l'}^{(i)}$, the posterior probability (121) is equal to that for the scalar AWGN channel (20). Thus, the MSE (123) and the posterior variance (124) coincide with each other for iteration i . This observation implies $\text{sir}_{l'}^{(i+1)} = \tilde{\text{sir}}_{l'}^{(i+1)}$, given by (26) for iteration $i + 1$.

APPENDIX B PROOF OF LEMMA 4

Let $\hat{u}(\tilde{x}, t) = u(\gamma \tilde{x}, t)$ for $\tilde{x} \in [-\gamma^{-1}, \gamma^{-1}]$. We first show that the partial differential equation (62) is represented as

$$\frac{\partial \hat{u}}{\partial t} = -A(\hat{u}(\tilde{x}, t)) \frac{\delta H}{\delta \hat{u}} [\hat{u}(\cdot, t)](\tilde{x}), \quad (126)$$

with some energy functional H . In (126), $\delta/\delta \hat{u}$ denotes the functional (Fréchet) derivative with respect to \hat{u} . Furthermore, the boundary condition $\hat{u}(\pm \gamma^{-1}, t) = u_{\max}$ is imposed.

Let us define the energy functional H as

$$H[\hat{u}] = \int_{-\gamma^{-1}}^{\gamma^{-1}} \left[V(\hat{u}(\tilde{x})) + \frac{B(\hat{u}(\tilde{x}))}{2} \left(\frac{\partial \hat{u}}{\partial \tilde{x}} \right)^2 \right] d\tilde{x}. \quad (127)$$

For functions $\hat{u}(\tilde{x})$ and $w(\tilde{x})$, we expand the energy functional $H[\hat{u} + \epsilon w]$, given by (127), around $\epsilon = 0$ to obtain

$$H[\hat{u} + \epsilon w] = H[\hat{u}] + \epsilon \frac{\partial H}{\partial \epsilon} [\hat{u}] + O(\epsilon^2), \quad (128)$$

with

$$\begin{aligned} \frac{\partial H}{\partial \epsilon} [\hat{u}] &= \int_{-\gamma^{-1}}^{\gamma^{-1}} \left[V'(\hat{u}(\tilde{x})) + \frac{B'(\hat{u}(\tilde{x}))}{2} \left(\frac{\partial \hat{u}}{\partial \tilde{x}} \right)^2 \right] w(\tilde{x}) d\tilde{x} \\ &\quad + \int_{-\gamma^{-1}}^{\gamma^{-1}} B(\hat{u}(\tilde{x})) \frac{\partial \hat{u}}{\partial \tilde{x}} \frac{\partial w}{\partial \tilde{x}} d\tilde{x}. \end{aligned} \quad (129)$$

Since $\hat{u}(\tilde{x}) + \epsilon w(\tilde{x})$ must satisfy the boundary conditions $\hat{u}(\pm \gamma^{-1}) + \epsilon w(\pm \gamma^{-1}) = u_{\max}$ around $\epsilon = 0$, we impose the boundary conditions $\hat{u}(\pm \gamma^{-1}) = u_{\max}$ and $w(\pm \gamma^{-1}) = 0$. Integrating by parts the last term in (129) with the boundary condition $w(\pm \gamma^{-1}) = 0$ yields

$$\frac{\partial H}{\partial \epsilon} [\hat{u}] = \int_{-\gamma^{-1}}^{\gamma^{-1}} \{ V'(\hat{u}(\tilde{x})) - \mathcal{L}[\hat{u}](\tilde{x}) \} w(\tilde{x}) d\tilde{x}, \quad (130)$$

with \mathcal{L} defined in (60). This expression implies that the functional derivative of (127) is given by

$$\frac{\delta H}{\delta \hat{u}} [\hat{u}](\tilde{x}) = V'(\hat{u}(\tilde{x})) - \mathcal{L}[\hat{u}](\tilde{x}). \quad (131)$$

Substituting (131) into (126), we find that (126) is equal to (62) under the change of variables $x = \gamma \tilde{x}$.

We next show that

$$\frac{dH}{dt} [\hat{u}(\cdot, t)] = - \int_{-\gamma^{-1}}^{\gamma^{-1}} A(\hat{u}(\tilde{x}, t)) \left(\frac{\delta H}{\delta \hat{u}} [\hat{u}(\cdot, t)](\tilde{x}) \right)^2 d\tilde{x} \leq 0, \quad (132)$$

where the equality holds if and only if $\delta H/\delta \hat{u} = 0$, since $A(\cdot)$ given by (63) is a positive function. This implies that the energy functional (127) is a Lyapunov functional [55] on the space of twice continuously differentiable functions with the norm $\|u\| = \|u\|_{\infty} + \|u'\|_{\infty} + \|u''\|_{\infty}$. The space is known to be complete with respect to this norm. Lyapunov's direct method implies that Lemma 4 follows from (132). The detailed proof is omitted since it is beyond the scope of this paper.

Intuitively, the energy functional (127) monotonically decreases with the time-evolution of the state. Since (127) is bounded below, $H[\hat{u}(\cdot, t)]$ converges to a finite value as $t \rightarrow \infty$, where $dH/dt = 0$ holds and thus the functional derivative $\delta H/\delta \hat{u}$ vanishes. As $\gamma \rightarrow 0$ the problem (126) for the interval $[-\gamma^{-1}, \gamma^{-1}]$ reduces to that for the infinite interval $(-\infty, \infty)$. Nonetheless, the argument above should be valid as $\gamma \rightarrow 0$, although a careful treatment for the region $|\tilde{x}| \gg 1$ is required in considering the energy functional (127) and the functional derivative (132). These intuitive arguments

imply that as $t \rightarrow \infty$ the state $\hat{u}(\tilde{x}, t)$ should converge uniformly to a stationary state with respect to $\gamma > 0$.

Let us prove (132). Differentiating (127) yields

$$\begin{aligned} \frac{dH}{dt}[\hat{u}(\cdot, t)] &= \int_{-\gamma^{-1}}^{\gamma^{-1}} \left[V'(\hat{u}(\tilde{x}, t)) + \frac{B'(\hat{u}(\tilde{x}, t))}{2} \left(\frac{\partial \hat{u}}{\partial \tilde{x}} \right)^2 \right] \frac{\partial \hat{u}}{\partial t} d\tilde{x} \\ &\quad + \int_{-\gamma^{-1}}^{\gamma^{-1}} B(\hat{u}(\tilde{x}, t)) \frac{\partial \hat{u}}{\partial \tilde{x}} \frac{\partial^2 \hat{u}}{\partial t \partial \tilde{x}} d\tilde{x}. \end{aligned} \quad (133)$$

Integrating by parts the last term, we obtain

$$\frac{dH}{dt}[\hat{u}(\cdot, t)] = \int_{-\gamma^{-1}}^{\gamma^{-1}} \frac{\delta H}{\delta \hat{u}}[\hat{u}(\cdot, t)](\tilde{x}) \frac{\partial \hat{u}}{\partial t} d\tilde{x}, \quad (134)$$

with (131), where we have used $\partial u(\pm \gamma^{-1}, t)/\partial t = 0$, which is obtained from the boundary condition $\hat{u}(\pm \gamma^{-1}, t) = u_{\max}$. Substituting (126) into (134) yields (132).

APPENDIX C PROOF OF LEMMA 5

In order to explain the idea for proving Lemma 5, let us discretize the time derivative in (66) as $\partial \tilde{v}/\partial t \approx (\tilde{v}(x, t+\delta) - \tilde{v}(x, t))/\delta$ for small $\delta > 0$. The differential system (66) is approximated by the discrete-time system $\tilde{v}_{n+1}(x) = \delta \mathfrak{G}[\tilde{v}_n(\cdot)](x)$ for $n \in \mathbb{N}$, i.e. $\tilde{v}(x, n\delta) \approx \tilde{v}_n(x)$. Proposition 3 implies that, for sufficiently small $\gamma > 0$, finite iterations of the system should result in a negligibly small change of the state $\tilde{v}_n(x)$ when the initial function $\tilde{v}_0(x)$ is smooth and very close to the solution $v_\gamma(x)$ of the fixed-point equation $v_\gamma(x) = \mathfrak{G}[v_\gamma(\cdot)](x)$. Since $\tilde{v}(x, t_0) \approx \tilde{v}_{n_0}(x)$ for $n_0 = t_0/\delta$, the state of the differential system (66) at time $t = t_0$ should be very close to the initial state as long as t_0 is finite. The proof of Lemma 5 is based on this intuition.

Let $\tilde{v}_n(x) = \tilde{v}(x, \delta n)$ for $\delta > 0$. We define two coupled sequences $\epsilon_n(x)$ and $\rho_n(x)$ of functions for $x \in \mathbb{R}$ by

$$\epsilon_n(x) = \delta \{ \rho_n(x) + (\kappa_n(x) + \epsilon_1) \chi_{[-1,1]}(x) \}, \quad (135)$$

$$\rho_{n+1}(x) = \rho_n(x) + A \overline{\epsilon_n(x)} + \epsilon_n(x), \quad (136)$$

for $A > 0$ and $\epsilon_1 > 0$, with

$$\overline{\epsilon_n(x)} = \frac{1}{(2\gamma)^2} \int_{[-\gamma, \gamma]^2} \epsilon_n(x + \omega_1 + \omega_2) d\omega_1 d\omega_2. \quad (137)$$

In (135), $\chi_{[-1,1]}(x)$ denotes the indicator function of the interval $[-1, 1] \subset \mathbb{R}$, and the function $\kappa_n(x)$ is given by

$$\kappa_n(x) = \left| \mathfrak{G}[\tilde{v}(\cdot, \delta n)](x) - \tilde{\mathfrak{G}}[\tilde{v}(\cdot, \delta n)](x) \right|. \quad (138)$$

Since A and ϵ_1 are contained in (135) and (136), we note that $\epsilon_n(x)$ and $\rho_n(x)$ depend on A and ϵ_1 . We first prove the following lemma.

Lemma 7: For any $x \in [-1, 1]$, $\epsilon_0 > 0$, and any $\epsilon_1 > 0$, there exist some $A > 0$ and $\delta > 0$ such that

$$|\tilde{v}_n(x) - \mathfrak{G}[\tilde{v}_n](x)| < \rho_n(x), \quad (139)$$

$$|\tilde{v}_{n+1}(x) - \tilde{v}_n(x)| < \epsilon_n(x), \quad (140)$$

with $\rho_0(x) = \epsilon_0 \chi_{[-1,1]}(x)$.

Proof: Since we focus on $x \in [-1, 1]$, $\chi_{[-1,1]}(x) = 1$ holds. We first prove that the latter bound (140) is correct if the former bound (139) holds. We use the mean-value theorem [51] to find that for any $\epsilon_1 > 0$ there exists some $\delta > 0$ such that

$$|\tilde{v}(x, t+\delta) - \tilde{v}(x, t)| < \delta \left| \frac{\partial}{\partial t} \tilde{v}(x, t) \right| + \delta \epsilon_1. \quad (141)$$

From (66) and (141), we obtain

$$\begin{aligned} |\tilde{v}_{n+1}(x) - \tilde{v}_n(x)| &< \delta |\tilde{v}_n(x) - \mathfrak{G}[\tilde{v}_n](x)| + \delta \epsilon_1 \\ &< \delta \left\{ |\tilde{v}_n(x) - \mathfrak{G}[\tilde{v}_n](x)| + |\mathfrak{G}[\tilde{v}_n](x) - \tilde{\mathfrak{G}}[\tilde{v}_n](x)| + \epsilon_1 \right\}, \end{aligned} \quad (142)$$

which implies that the latter bound (140) holds if the former bound (139) is correct.

The proof is by induction. For $n = 0$ (139) holds by selecting sufficiently small $\epsilon_{\text{init}} > 0$, because of $|v_{\text{init}}(x) - v_\gamma(x, \infty)| < \epsilon_{\text{init}}$. Thus, the latter bound (140) is also correct. Suppose that (139) holds for some n . Thus, the latter bound (140) is correct. Using the triangle inequality yields

$$\begin{aligned} |\tilde{v}_{n+1}(x) - \mathfrak{G}[\tilde{v}_{n+1}](x)| &< |\tilde{v}_{n+1}(x) - \tilde{v}_n(x)| + |\tilde{v}_n(x) - \mathfrak{G}[\tilde{v}_n](x)| \\ &\quad + |\mathfrak{G}[\tilde{v}_n](x) - \mathfrak{G}[\tilde{v}_{n+1}](x)|. \end{aligned} \quad (143)$$

Since the functions φ and ψ are continuously differentiable, they are Lipschitz-continuous—there exist some positive constants $L_\varphi > 0$ and $L_\psi > 0$ such that $|\varphi(u_1) - \varphi(u_2)| < L_\varphi |u_1 - u_2|$ and $|\psi(v_1) - \psi(v_2)| < L_\psi |v_1 - v_2|$ for all $u_1, u_2 \in \tilde{\mathcal{D}}$ and $v_1, v_2 \in \mathcal{D}$. From (140) and the definition of \mathfrak{G} given via (56) and (57), it is possible to prove that

$$\begin{aligned} |\mathfrak{G}[\tilde{v}_{n+1}](x) - \mathfrak{G}[\tilde{v}_n](x)| &< \frac{A}{(2\gamma)^2} \int_{[-\gamma, \gamma]^2} \epsilon_n(x + \omega_1 + \omega_2) d\omega_1 d\omega_2, \end{aligned} \quad (144)$$

with $A = \beta L_\varphi L_\psi$. This implies that the RHS of (143) is bounded from above by $\rho_{n+1}(x)$. By induction, (139) and (140) hold for any n . ■

We next prove that

$$\lim_{\gamma \rightarrow 0} \frac{1}{\delta} \int_{-1}^1 \sup_{n \leq n_0} \epsilon_n(x) dx = 0, \quad (145)$$

with $n_0 = t_0/\delta \in \mathbb{N}$. Lemma 5 follows immediately from (145). Using the triangle inequality and Lemma 7 yield

$$\begin{aligned} \int_{-1}^1 |\tilde{v}(x, t_0) - \tilde{v}(x, 0)| dx &< \sum_{n=0}^{n_0-1} \int_{-1}^1 |\tilde{v}_{n+1}(x) - \tilde{v}_n(x)| dx \\ &< \frac{t_0}{\delta} \int_{-1}^1 \sup_{n < n_0} \epsilon_n(x) dx, \end{aligned} \quad (146)$$

where we have used (140). Applying (145) to (146) implies that Lemma 5 holds.

In order to prove (145), we let

$$\hat{\rho}_n(\omega) = \int_{-\infty}^{\infty} \rho_n(x) e^{-i\omega x} dx, \quad (147)$$

$$\hat{\kappa}_n(\omega) = \int_{-1}^1 \kappa_n(x) e^{-i\omega x} dx. \quad (148)$$

Applying the Fourier transform to both sides of (136), and then substituting (135) into the obtained expression, we obtain

$$\hat{\rho}_{n+1}(\omega) = \hat{\rho}_n(\omega) + \delta \hat{C}_1(\omega) \left(\hat{\rho}_n(\omega) + \hat{\kappa}_n(\omega) + 2\epsilon_1 \frac{\sin \omega}{\omega} \right), \quad (149)$$

with

$$\hat{C}_1(\omega) = A \left(\frac{\sin \gamma \omega}{\gamma \omega} \right)^2 + 1. \quad (150)$$

Proposition 3 implies that for any $\epsilon > 0$ there exists some $\gamma_0 > 0$ such that $|\hat{\kappa}_n(\omega)| < \epsilon$ for all $\gamma \in (0, \gamma_0)$, $n \leq n_0$, and all $\omega \in \mathbb{R}$. Solving (149) yields

$$|\hat{\rho}_n(\omega)| \leq \epsilon_0 \left| \frac{\sin \omega}{\omega} \right| + \hat{C}_2(\omega) \left\{ \left(1 + \delta |\hat{C}_1(\omega)| \right)^n - 1 \right\}, \quad (151)$$

with

$$\hat{C}_2(\omega) = \epsilon + (\epsilon_0 + 2\epsilon_1) \left| \frac{\sin \omega}{\omega} \right|. \quad (152)$$

Using $n \leq n_0 = t_0/\delta$ and the well-known fact that the function $f(x) = (1+1/x)^x$ for $x > 0$ monotonically increases toward e , we obtain

$$|\hat{\rho}_n(\omega)| < \epsilon_0 \left| \frac{\sin \omega}{\omega} \right| + \hat{C}_2(\omega) \left(e^{t_0 |\hat{C}_1(\omega)|} - 1 \right). \quad (153)$$

Taking $\omega \rightarrow 0$ yields

$$\lim_{\omega \rightarrow 0} |\hat{\rho}_n(\omega)| < \epsilon_0 + (\epsilon + \epsilon_0 + 2\epsilon_1) \left(e^{t_0(A+1)} - 1 \right), \quad (154)$$

which implies $\lim_{\gamma \rightarrow 0} \sup_{n \leq n_0} \lim_{\omega \rightarrow 0} |\hat{\rho}_n(\omega)| = 0$. Since $\rho_n(x) \geq 0$, from (147) we arrive at

$$\lim_{\gamma \rightarrow 0} \int_{-1}^1 \sup_{n \leq n_0} \rho_n(x) dx = 0. \quad (155)$$

From (135), this implies (145).

APPENDIX D PROOF OF THEOREM 8

We start with proving the following lemma.

Lemma 8: Suppose that \tilde{u}_r is the metastable solution of the effective potential $U(\tilde{u})$. If there is a solution $\tilde{u}(0) \in (\tilde{u}_1, \tilde{u}_{\text{un}})$ to the fixed-point equation $F(\tilde{u}(0)) = 1/\gamma$, with

$$F(x) = \int_x^{\tilde{u}_r} \frac{dy}{\sqrt{2\{U(y) - U(\tilde{u}(0))\}}}, \quad (156)$$

then there is a non-uniform stationary solution $\tilde{u}(x)$ to (90). Furthermore, the solution $\tilde{u}(x)$ satisfies

$$F(\tilde{u}(x)) = \frac{1 - |x|}{\gamma}. \quad (157)$$

Proof of Lemma 8: We confirm that $\tilde{u}(x)$ satisfying (157) is a stationary solution to (90). It is obvious that the solution (157) satisfies the boundary condition $\tilde{u}(\pm 1) = \tilde{u}_r$. Let us show that the solution (157) is a solution to (93). Differentiating (157) with respect to x yields

$$\frac{\gamma}{\sqrt{2}} \frac{d\tilde{u}}{dx} = \begin{cases} \sqrt{U(\tilde{u}) - U(\tilde{u}(0))} & \text{for } x > 0 \\ -\sqrt{U(\tilde{u}) - U(\tilde{u}(0))} & \text{for } x < 0, \end{cases} \quad (158)$$

which is equivalent to (93) with the constant $C = -U(\tilde{u}(0))$. Furthermore, it is straightforward to show that the LHS of (158) is differentiable with respect to x . These observations imply that the solution (157) is indeed a non-uniform stationary solution to (90). ■

Remark 6: The conservation of mechanical energy explains why $\tilde{u}(0)$ must be between \tilde{u}_1 and \tilde{u}_{un} , as defined in Lemma 8. Let us assume that there is a solution $\tilde{u}(x)$ to the Newton equation (92) such that the solution is on the right maximum of the inverted potential $-U(\tilde{u})$ at $x = -1$, and arrives at some position $\tilde{u}(0) > \tilde{u}_{\text{un}}$ at $x = 0$. The velocity $u'(0)$ at $x = 0$ must be zero, because of the differentiability of $\tilde{u}(x)$ at $x = 0$. However, the definition of \tilde{u}_{un} , i.e. $U(\tilde{u}_{\text{un}}) = U(\tilde{u}_r)$ implies $-U(\tilde{u}(0)) < -U(\tilde{u}_r)$, which breaks the conservation of mechanical energy:

$$\frac{\gamma^2}{2} \tilde{u}'(0)^2 - U(\tilde{u}(0)) < \frac{\gamma^2}{2} \tilde{u}'(-1)^2 - U(\tilde{u}_r). \quad (159)$$

Thus, $\tilde{u}(0)$ must be smaller than \tilde{u}_{un} .

The same argument explains that $\tilde{u}(0)$ must be larger than \tilde{u}_1 . Let us assume $\tilde{u}(0) < \tilde{u}_1$. Then, the conservation of mechanical energy implies that the velocity $\tilde{u}'(0)$ at $x = 0$ must be non-zero, since \tilde{u}_1 is the global maximizer of the inverted potential $-U(\tilde{u})$. However, the non-zero velocity $\tilde{u}'(0)$ contradicts the differentiability of $\tilde{u}(x)$ at $x = 0$. Thus, $\tilde{u}(0)$ must be larger than \tilde{u}_1 . From the arguments above, $\tilde{u}(0)$ must be between \tilde{u}_1 and \tilde{u}_{un} .

In order to prove the first part of Theorem 8, we show that $F(\tilde{u}(0))$ is bounded for all $\tilde{u}(0) \in (\tilde{u}_1, \tilde{u}_{\text{un}})$, and that $F(\tilde{u}(0))$ tends to infinity as $\tilde{u}(0) \rightarrow \tilde{u}_1$ or as $\tilde{u}(0) \rightarrow \tilde{u}_{\text{un}}$. Lemma 8 and these properties of $F(\tilde{u}(0))$ imply that there are two non-uniform stationary solutions to (90) for sufficiently small $\gamma > 0$.

We shall show the former property of $F(\tilde{u}(0))$. Let \tilde{u}_0 denote a value between $\tilde{u}(0)$ and the unstable solution of the effective potential $U(\tilde{u})$. Splitting the interval of integration $(\tilde{u}(0), \tilde{u}_r)$ into the two intervals $(\tilde{u}(0), \tilde{u}_0)$ and $(\tilde{u}_0, \tilde{u}_r)$ yields

$$F(\tilde{u}(0)) = \int_{\tilde{u}(0)}^{\tilde{u}_0} \frac{dy}{\sqrt{2\{U(y) - U(\tilde{u}(0))\}}} + \int_{\tilde{u}_0}^{\tilde{u}_r} \frac{dy}{\sqrt{2\{U(y) - U(\tilde{u}(0))\}}}. \quad (160)$$

The condition $\tilde{u}(0) < \tilde{u}_{\text{un}}$ implies that the second term is bounded, because of $U(y) > U(\tilde{u}(0))$ for all $y \in [\tilde{u}_0, \tilde{u}_r]$. Thus, we focus on the first term. Let \tilde{u} denote an appropriately chosen value between $\tilde{u}(0)$ and \tilde{u}_0 . From the mean-value

theorem [51], we obtain

$$\begin{aligned}
& \int_{\tilde{u}(0)}^{\tilde{u}_0} \frac{dy}{\sqrt{2\{U(y) - U(\tilde{u}(0))\}}} \\
&= \int_{\tilde{u}(0)}^{\tilde{u}_0} \frac{dy}{\sqrt{2U'(\tilde{u})(y - \tilde{u}(0))}} \\
&< \sup_{\tilde{u} \in (\tilde{u}(0), \tilde{u}_0)} \frac{1}{\sqrt{U'(\tilde{u})}} \int_{\tilde{u}(0)}^{\tilde{u}_0} \frac{dy}{\sqrt{2(y - \tilde{u}(0))}} \\
&= \sqrt{2(\tilde{u}_0 - \tilde{u}(0))} \sup_{\tilde{u} \in (\tilde{u}(0), \tilde{u}_0)} \frac{1}{\sqrt{U'(\tilde{u})}}, \quad (161)
\end{aligned}$$

which is bounded, because of $\tilde{u}(0) > \tilde{u}_1$. Thus, we find that $F(\tilde{u}(0))$ is bounded for all $\tilde{u}(0) \in (\tilde{u}_1, \tilde{u}_{\text{un}})$.

We next show the latter property of $F(\tilde{u}(0))$. The upper bound (161) on the first term of (160) diverges as $\tilde{u}(0) \rightarrow \tilde{u}_1$, because of $U'(\tilde{u}_1) = 0$. It is straightforward to show that the first term of (160) tends to infinity as $\tilde{u}(0) \rightarrow \tilde{u}_1$. On the other hand, the second term of (160) diverges as $\tilde{u}(0) \rightarrow \tilde{u}_{\text{un}}$, owing to $U(\tilde{u}_r) = U(\tilde{u}_{\text{un}})$. These observations imply that $\tilde{u}(0) = \tilde{u}_1$ and $\tilde{u}(0) = \tilde{u}_{\text{un}}$ are solutions to the fixed-point equation $F(\tilde{u}(0)) = 1/\gamma$ in the limit $\gamma \rightarrow 0$.

We have shown that there are two non-uniform stationary solutions $\tilde{u}_s(x)$ and $\tilde{u}_{\text{un}}(x)$ to (90) for sufficiently small $\gamma > 0$, and that $\tilde{u}_s(0)$ and $\tilde{u}_{\text{un}}(0)$ tend to \tilde{u}_1 and \tilde{u}_{un} in the limit $\gamma \rightarrow 0$, respectively. We next prove that $\tilde{u}_s(x)$ converges to \tilde{u}_1 for $x \in (-1, 1)$ in the limit $\gamma \rightarrow 0$, and that $\tilde{u}_{\text{un}}(x)$ tends to \tilde{u}_r for $x \neq 0$ in the limit $\gamma \rightarrow 0$. Since the stationary solutions are even functions, without loss of generality, we focus on the interval $(0, 1]$. Differentiating (157) for $x \in (0, 1]$ with respect to x yields

$$\frac{\tilde{u}'(x)}{\sqrt{2\{U(\tilde{u}(x)) - U(\tilde{u}(0))\}}} = \frac{1}{\gamma}, \quad (162)$$

where we have used (156). For the stationary solution $\tilde{u}(x) = \tilde{u}_s(x)$, the denominator on the LHS of (162) should tend to zero as $\gamma \rightarrow 0$. Since \tilde{u}_1 is the global stable solution of the potential $U(\tilde{u})$, the stationary solution $\tilde{u}_s(x)$ tends to $\tilde{u}(0) = \tilde{u}_1$ for $x \in (0, 1]$ in the limit $\gamma \rightarrow 0$. Similarly, we find that $\tilde{u}_{\text{un}}(x)$ converges to \tilde{u}_r or \tilde{u}_{un} for $x \in (0, 1]$ in the limit $\gamma \rightarrow 0$, because of $U(\tilde{u}_{\text{un}}) = U(\tilde{u}_r)$.

We shall prove the convergence of $\tilde{u}_{\text{un}}(x)$ toward \tilde{u}_r for $x \in (0, 1]$ in the limit $\gamma \rightarrow 0$. For that purpose, we show $\tilde{u}_{\text{un}}(x) > \tilde{u}_{\text{un}}$ for $x \in (0, \epsilon)$, with sufficiently small $\epsilon > 0$. Combining this property and $\tilde{u}'_{\text{un}}(x) \geq 0$ for $x \in (0, 1]$, obtained from (162), we find $\tilde{u}_{\text{un}}(x) > \tilde{u}_{\text{un}}$ for $x \in (0, 1]$. This implies that $\tilde{u}_{\text{un}}(x)$ tends to \tilde{u}_r for $x \in (0, 1]$ in the limit $\gamma \rightarrow 0$.

Let us prove $\tilde{u}_{\text{un}}(x) > \tilde{u}_{\text{un}}$ for $x \in (0, \epsilon)$, for sufficiently small $\epsilon > 0$. The mean-value theorem implies

$$\tilde{u}'_{\text{un}}(x) = \tilde{u}'_{\text{un}}(0) + \tilde{u}''_{\text{un}}(\bar{x})x, \quad (163)$$

for $x \in (0, \epsilon)$ and some $\bar{x} \in (0, x)$. Substituting $\tilde{u}'_{\text{un}}(0) = 0$ and (92) into (163), we obtain

$$\tilde{u}'_{\text{un}}(x) = \frac{U'(\tilde{u}_{\text{un}}(\bar{x}))}{\gamma^2}x. \quad (164)$$

This expression implies that $\tilde{u}'_{\text{un}}(x)$ is strictly positive for $x \in (0, \epsilon)$, because of $U'(\tilde{u}_{\text{un}}(\bar{x})) > 0$. Thus, we find

$\tilde{u}_{\text{un}}(x) > \tilde{u}_{\text{un}}(0) = \tilde{u}_{\text{un}}$ in the neighborhood $(0, \epsilon)$. This observation corresponds to the physical fact that a free particle cannot continue to stay at a point on a smooth slope.

We complete the proof of Theorem 8, by analyzing the stability of the non-uniform stationary solution $\tilde{u}_s(x)$ in the limit $\gamma \rightarrow 0$. Repeating the derivation of (86), we find that (90) can be represented as

$$\frac{\partial \tilde{u}}{\partial t} = -A(g^{-1}(\tilde{u}))B(g^{-1}(\tilde{u}))\frac{\delta \tilde{H}}{\delta \tilde{u}}[\tilde{u}(\cdot, t)](x), \quad (165)$$

with

$$\tilde{H}[\tilde{u}] = \int_{-1}^1 \left[U(\tilde{u}(x)) + \frac{\gamma^2}{2} \left(\frac{\partial \tilde{u}}{\partial x} \right)^2 \right] dx. \quad (166)$$

Since $A(u)$ and $B(u)$ are positive, $\tilde{u}_s(x)$ is stable if $\tilde{u}_s(x)$ is a (local) minimizer of the energy functional (166). We shall prove

$$\lim_{\gamma \rightarrow 0} \tilde{H}[\tilde{u}_s] = 2U(\tilde{u}_1), \quad (167)$$

which implies that $\tilde{u}_s(x)$ attains the global minimum of (166) in the limit $\gamma \rightarrow 0$, since \tilde{u}_1 is the global stable solution of the potential $U(\tilde{u})$. Thus, the solution $\tilde{u}_s(x)$ is stable in the limit $\gamma \rightarrow 0$.

Let us prove (167). Substituting (158) into (166) yields

$$\tilde{H}[\tilde{u}_s] = 2 \int_{-1}^1 U(\tilde{u}_s(x))dx - 2U(\tilde{u}_s(0)). \quad (168)$$

Since the integrand $U(\tilde{u}_s(x))$ is obviously bounded for all $x \in [-1, 1]$, the dominated convergence theorem implies

$$\lim_{\gamma \rightarrow 0} \tilde{H}[\tilde{u}_s] = 2 \int_{-1}^1 \lim_{\gamma \rightarrow 0} U(\tilde{u}_s(x))dx - 2U(\tilde{u}_1) = 2U(\tilde{u}_1), \quad (169)$$

where we have used the fact that $\tilde{u}_s(x)$ converges to \tilde{u}_1 for $x \in (-1, 1)$ in the limit $\gamma \rightarrow 0$.

ACKNOWLEDGMENT

The authors thank the anonymous reviewers for their suggestions that have improved the quality of the manuscript greatly. In addition, the authors are grateful to Hiroshi Nagaoka for useful comments on the proof of Theorem 5.

REFERENCES

- [1] F. Adachi, M. Sawahashi, and H. Suda, "Wideband DS-CDMA for next-generation mobile communications systems," *IEEE Commun. Mag.*, vol. 36, no. 9, pp. 56–69, Sep. 1998.
- [2] E. Dahlman, B. Gudmundson, M. Nilsson, and J. Sköld, "UMTS/IMT-2000 based on wideband CDMA," *IEEE Commun. Mag.*, vol. 36, no. 9, pp. 70–80, Sep. 1998.
- [3] T. Ojanperä and R. Prasad, "An overview of air interface multiple access for IMT-2000/UMTS," *IEEE Commun. Mag.*, vol. 36, no. 9, pp. 82–86 and 91–95, Sep. 1998.
- [4] S. Verdú, *Multuser Detection*. New York, NY, USA: Cambridge Univ. Press, 1998.
- [5] R. Lupas and S. Verdú, "Linear multiuser detectors for synchronous code-division multiple-access channels," *IEEE Trans. Inf. Theory*, vol. 35, no. 1, pp. 123–136, Jan. 1989.
- [6] Z. Xie, R. T. Short, and C. K. Rushforth, "A family of suboptimum detectors for coherent multiuser communications," *IEEE J. Sel. Areas Commun.*, vol. 8, no. 4, pp. 683–690, May 1990.

- [7] U. Madhow and M. L. Honig, "MMSE interference suppression for direct-sequence spread-spectrum CDMA," *IEEE Trans. Commun.*, vol. 42, no. 12, pp. 3178–3188, Dec. 1994.
- [8] D. N. C. Tse and S. V. Hanly, "Linear multiuser receivers: Effective interference, effective bandwidth and user capacity," *IEEE Trans. Inf. Theory*, vol. 45, no. 2, pp. 641–657, Mar. 1999.
- [9] S. Verdú and S. Shamai (Shitz), "Spectral efficiency of CDMA with random spreading," *IEEE Trans. Inf. Theory*, vol. 45, no. 2, pp. 622–640, Mar. 1999.
- [10] T. Tanaka, "A statistical-mechanics approach to large-system analysis of CDMA multiuser detectors," *IEEE Trans. Inf. Theory*, vol. 48, no. 11, pp. 2888–2910, Nov. 2002.
- [11] R. Müller and W. H. Gerstacker, "On the capacity loss due to separation of detection and decoding," *IEEE Trans. Inf. Theory*, vol. 50, no. 8, pp. 1769–1778, Aug. 2004.
- [12] D. Guo and S. Verdú, "Randomly spread CDMA: Asymptotics via statistical physics," *IEEE Trans. Inf. Theory*, vol. 51, no. 6, pp. 1983–2010, Jun. 2005.
- [13] J. Pearl, *Probabilistic Reasoning in Intelligent Systems: Networks of Plausible Inference*. San Francisco, CA, USA: Morgan Kaufmann, 1988.
- [14] T. Richardson and R. Urbanke, *Modern Coding Theory*. New York, NY, USA: Cambridge Univ. Press, 2008.
- [15] X. Wang and H. V. Poor, "Iterative (turbo) soft interference cancellation and decoding for coded CDMA," *IEEE Trans. Commun.*, vol. 47, no. 7, pp. 1046–1061, Jul. 1999.
- [16] J. Boutros and G. Caire, "Iterative multiuser joint decoding: Unified framework and asymptotic analysis," *IEEE Trans. Inf. Theory*, vol. 48, no. 7, pp. 1772–1793, Jul. 2002.
- [17] G. Caire, R. Müller, and T. Tanaka, "Iterative multiuser joint decoding: Optimal power allocation and low-complexity implementation," *IEEE Trans. Inf. Theory*, vol. 50, no. 9, pp. 1950–1973, Sep. 2004.
- [18] Y. Kabashima, "A CDMA multiuser detection algorithm on the basis of belief propagation," *J. Phys. A, Math. General*, vol. 36, no. 43, pp. 11111–11121, Oct. 2003.
- [19] K. Takeuchi and S. Horio, "Iterative multiuser detection and decoding with spatially coupled interleaving," *IEEE Wireless Commun. Lett.*, vol. 2, no. 6, pp. 619–622, Dec. 2013.
- [20] A. Montanari and D. Tse, "Analysis of belief propagation for non-linear problems: The example of CDMA (or: How to prove Tanaka's formula)," in *Proc. IEEE Inf. Theory Workshop*, Punta del Este, Uruguay, Mar. 2006, pp. 160–164.
- [21] M. Yoshida and T. Tanaka, "Analysis of sparsely-spread CDMA via statistical mechanics," in *Proc. IEEE Int. Symp. Inf. Theory*, Seattle, WA, USA, Jul. 2006, pp. 2378–2382.
- [22] J. Raymond and D. Saad, "Sparsely spread CDMA—A statistical mechanics-based analysis," *J. Phys. A, Math. Theoretical*, vol. 40, no. 41, pp. 12315–12333, Oct. 2007.
- [23] D. Guo and C.-C. Wang, "Multiuser detection of sparsely spread CDMA," *IEEE J. Sel. Areas Commun.*, vol. 26, no. 3, pp. 421–431, Apr. 2008.
- [24] S. Kudekar, T. J. Richardson, and R. L. Urbanke, "Threshold saturation via spatial coupling: Why convolutional LDPC ensembles perform so well over the BEC," *IEEE Trans. Inf. Theory*, vol. 57, no. 2, pp. 803–834, Feb. 2011.
- [25] A. Jimenez Felstrom and K. S. Zigangirov, "Time-varying periodic convolutional codes with low-density parity-check matrix," *IEEE Trans. Inf. Theory*, vol. 45, no. 6, pp. 2181–2191, Sep. 1999.
- [26] M. Lentmaier and G. P. Fettweis, "On the thresholds of generalized LDPC convolutional codes based on protographs," in *Proc. IEEE Int. Symp. Inf. Theory*, Austin, TX, USA, Jun. 2010, pp. 709–713.
- [27] S. H. Hassani, N. Macris, and R. Urbanke, "Coupled graphical models and their thresholds," in *Proc. IEEE Inf. Theory Workshop*, Dublin, Ireland, Aug./Sep. 2010, pp. 1–5.
- [28] S. H. Hassani, N. Macris, and R. Urbanke, "Chains of mean-field models," *J. Statist. Mech., Theory Experim.*, vol. 2012, no. 2, p. P02011, Feb. 2012.
- [29] K. Takeuchi, T. Tanaka, and T. Kawabata, "A phenomenological study on threshold improvement via spatial coupling," *IEICE Trans. Fundam. Electron., Commun. Comput. Sci.*, vol. E95-A, no. 5, pp. 974–977, May 2012.
- [30] A. Yedla, Y.-Y. Jian, P. S. Nguyen, and H. D. Pfister, "A simple proof of threshold saturation for coupled scalar recursions," in *Proc. 7th Int. Symp. Turbo Codes Iterative Inf. Process.*, Gothenburg, Sweden, Aug. 2012, pp. 51–55.
- [31] S. Kudekar, T. Richardson, and R. Urbanke, "Wave-like solutions of general one-dimensional spatially coupled systems," *IEEE Trans. Inf. Theory*, to be published. [Online]. Available: <http://arxiv.org/abs/1208.5273>
- [32] C. Schlegel and M. Burnashev, "Thresholds of spatially coupled systems via Lyapunov's method," in *Proc. IEEE Inf. Theory Workshop*, Sevilla, Spain, Sep. 2013, pp. 1–5.
- [33] S. Kudekar and H. D. Pfister, "The effect of spatial coupling on compressive sensing," in *Proc. 48th Annu. Allerton Conf. Commun. Control, Comput.*, Los Alamos, NM, USA, Sep./Oct. 2010, pp. 347–353.
- [34] F. Krzakala, M. Mézard, F. Sausset, Y. F. Sun, and L. Zdeborová, "Statistical-physics-based reconstruction in compressed sensing," *Phys. Rev. X*, vol. 2, no. 2, pp. 021005–1–021005-18, May 2012.
- [35] D. L. Donoho, A. Javanmard, and A. Montanari, "Information-theoretically optimal compressed sensing via spatial coupling and approximate message passing," *IEEE Trans. Inf. Theory*, vol. 59, no. 11, pp. 7434–7464, Nov. 2013.
- [36] M. Hagiwara, K. Kasai, H. Imai, and K. Sakaniwa, "Spatially coupled quasi-cyclic quantum LDPC codes," in *Proc. IEEE Int. Symp. Inf. Theory*, St. Petersburg, Russia, Aug. 2011, pp. 638–642.
- [37] K. Kasai and K. Sakaniwa, "Spatially-coupled MacKay–Neal codes and Hsu–Anastasopoulos codes," *IEICE Trans. Fundam. Electron., Commun. Comput. Sci.*, vol. E94-A, no. 11, pp. 2161–2168, Nov. 2011.
- [38] S. Kudekar and K. Kasai, "Threshold saturation on channels with memory via spatial coupling," in *Proc. IEEE Int. Symp. Inf. Theory*, St. Petersburg, Russia, Aug. 2011, pp. 2562–2566.
- [39] S. Kudekar and K. Kasai, "Spatially coupled codes over the multiple access channel," in *Proc. IEEE Int. Symp. Inf. Theory*, St. Petersburg, Russia, Aug. 2011, pp. 2816–2820.
- [40] V. Rathi, R. Urbanke, M. Andersson, and M. Skoglund, "Rate-equivocation optimal spatially coupled LDPC codes for the BEC wiretap channel," in *Proc. IEEE Int. Symp. Inf. Theory*, St. Petersburg, Russia, Aug. 2011, pp. 2393–2397.
- [41] C. Schlegel and D. Truhachev, "Multiple access demodulation in the lifted signal graph with spatial coupling," in *Proc. IEEE Int. Symp. Inf. Theory*, St. Petersburg, Russia, Aug. 2011, pp. 2989–2993.
- [42] C. Schlegel and D. Truhachev, "Multiple access demodulation in the lifted signal graph with spatial coupling," *IEEE Trans. Inf. Theory*, vol. 59, no. 4, pp. 2459–2470, Apr. 2013.
- [43] K. Takeuchi, T. Tanaka, and T. Kawabata, "Improvement of BP-based CDMA multiuser detection by spatial coupling," in *Proc. IEEE Int. Symp. Inf. Theory*, St. Petersburg, Russia, Aug. 2011, pp. 1489–1493.
- [44] H. Uchikawa, K. Kasai, and K. Sakaniwa, "Spatially coupled LDPC codes for decode-and-forward in erasure relay channel," in *Proc. IEEE Int. Symp. Inf. Theory*, St. Petersburg, Russia, Aug. 2011, pp. 1474–1478.
- [45] A. Yedla, H. D. Pfister, and K. R. Narayanan, "Universality for the noisy Slepian–Wolf problem via spatial coupling," in *Proc. IEEE Int. Symp. Inf. Theory*, St. Petersburg, Russia, Aug. 2011, pp. 2567–2571.
- [46] V. Aref and R. L. Urbanke, "Universal rateless codes from coupled LT codes," in *Proc. IEEE Inf. Theory Workshop*, Paraty, Brazil, Oct. 2011, pp. 277–281.
- [47] D. Truhachev, "Achieving AWGN multiple access channel capacity with spatial graph coupling," *IEEE Commun. Lett.*, vol. 16, no. 5, pp. 585–588, May 2012.
- [48] D. Guo, S. Shamai (Shitz), and S. Verdú, "Mutual information and minimum mean-square error in Gaussian channels," *IEEE Trans. Inf. Theory*, vol. 51, no. 4, pp. 1261–1282, Apr. 2005.
- [49] S. B. Korada and A. Montanari, "Applications of the Lindeberg principle in communications and statistical learning," *IEEE Trans. Inf. Theory*, vol. 57, no. 4, pp. 2440–2450, Apr. 2011.
- [50] R. B. Ash and C. A. Doléans-Dade, *Probability & Measure Theory*, 2nd ed. San Diego, CA, USA: Academic, 1999.
- [51] G. Strang, *Calculus*, 2nd ed. Wellesley, MA, USA: Wellesley-Cambridge, 2010.
- [52] S.-I. Amari and H. Nagaoka, *Methods of Information Geometry*. Providence, RI, USA: AMS, 2000.
- [53] S. Kobayashi and K. Nomizu, *Foundations of Differential Geometry*. New York, NY, USA: Wiley, 1996.
- [54] T. Ikehara and T. Tanaka, "Decoupling principle in belief-propagation-based CDMA multiuser detection algorithm," in *Proc. IEEE Int. Symp. Inf. Theory*, Nice, France, Jun. 2007, pp. 2081–2085.
- [55] A. N. Michel, L. Hou, and D. Liu, *Stability of Dynamical Systems: Continuous, Discontinuous, and Discrete Systems*. Boston, MA, USA: Birkhäuser, 2008.

Keigo Takeuchi (S'08–M'09) received the B. Eng., M. Inf., and Ph.D. degrees in informatics from Kyoto University, Kyoto, Japan, in 2004, 2006, and 2009, respectively.

Since 2009 he has been an Assistant Professor at the Department of Communication Engineering and Informatics, the University of Electro-Communications, Tokyo, Japan. He is serving as an Associate Editor of *IEICE Trans. Fundamentals*, from 2013. He held a visiting appointment at the Norwegian University of Science and Technology (NTNU), Norway. His research interests are in the field of wireless communications, statistical signal processing, and statistical-mechanical informatics. Dr. Takeuchi received the 2008 IEEE Kansai Section Student Paper Award for the paper "Asymptotic Analysis of General Multiuser Detectors in MIMO DS-CDMA Channels."

Toshiyuki Tanaka (S'90–M'93) received the B. Eng., M. Eng., and Dr. Eng. degrees in Electronics Engineering from the University of Tokyo, Tokyo, Japan, in 1988, 1990, and 1993, respectively.

From 1993 until 2005, he was with the Department of Electronics and Information Engineering at Tokyo Metropolitan University, Tokyo, Japan. In 2005, he moved to the Graduate School of Informatics, Kyoto University, Kyoto, Japan, where he is currently a professor. His research interests are in the areas of communication theory, statistical learning, and statistical mechanical informatics.

Dr. Tanaka received DoCoMo Mobile Science Prize in 2003, and Young Scientist Award from the Ministry of Education, Culture, Sports, Science and Technology, Japan, in 2005.

Tsutomu Kawabata (M'93) was born in Toyama, Japan, in 1955. He received BE, ME, and DE degrees in mathematical engineering from the University of Tokyo, in 1978, 1980, and 1993 respectively.

He joined the University of Electro-Communications in 1982 and is currently a Professor at the Department of Communication Engineering and Informatics. He was a visitor at Stanford University during 1987–89 and 1996–97, and at Eindhoven University of Technology in 1995, and at INRIA in 1996. His research interests lie in information and communication theory, and include quantizations, rate-distortions, and lossless data compressions.